Australian Government
Department of Defence
Defence Science and
Technology Organisation

Sep 2003

DSTO

Distributed-feedback (DFB) Laser Coherence and Linewidth Broadening

Linh V. T. Nguyen

DSTO-RR-0263

Australian Government
Department of Defence
Defence Science and
Technology Organisation

Distributed-feedback (DFB) Laser Coherence and Linewidth Broadening

Linh V T Nguyen

Electronic Warfare & Radar Division
Systems Sciences Laboratory

DSTO-RR-0263

ABSTRACT

The primary goal of the research activity presented in this report is to understand the range of applicability for different types of lasers to a variety of Electronic Warfare (EW) applications. This work provides a detailed investigation into laser coherence properties. In particular, the emphasis of this work was on linewidth broadening of commercial-of-the-shelf (COTS) distributed-feedback (DFB) semiconductor lasers, turning them into compatible sources for microwave photonic signal processing. Optical linewidth refers to the optical phase fluctuation of the lasing longitudinal modes. Laser devices having narrow linewidth are said to have a high degree of coherence.

The investigation into laser coherence properties includes linewidth measurements, using a phase-modulated delayed self-heterodyning method, of multi-mode Fabry-Perot (FP) and single-mode DFB semiconductor lasers. Leveraging from these measurements, a combination of injection dithering and external phase modulation is proposed to broaden the linewidth of a COTS DFB laser device. Linewidth broadening from 10 MHz to over 200 MHz is possible without splitting the linewidth distribution, which is often associated with wavelength chirping in semiconductor lasers. The linewidth broadening from 10 MHz to over 200 MHz corresponds to a reduction of laser coherence length from 20 metres to less than 1 metre in optical fibres. The advantages and limitations of the linewidth broadening technique and its applicability to microwave photonic signal processing in EW systems are addressed in this report.

Approved for Public Release

Published by

DSTO Systems Sciences Laboratory
PO Box 1500
Edinburgh South Australia 5111 Australia

Telephone: (08) 8259 5555
Fax: (08) 8259 6567

AR- 012-887
September 2003

APPROVED FOR PUBLIC RELEASE

Distributed-feedback (DFB) Laser Coherence and Linewidth Broadening

Executive Summary

Distributed-feedback (DFB) semiconductor lasers are single-mode devices operating at 1550 nm. There are favourable properties at this wavelength including low fibre attenuation, applicability of dense wavelength-division multiplexing (DWDM) techniques and erbium-doped fibre amplifiers (EDFAs). These DFB laser devices are also useful in microwave photonic signal processing for the same reasons. In addition, they manifest Gaussian power probability distribution, which is required to represent the statistical nature of target cross-section in Electronic Warfare (EW) receivers.

One critical drawback in the utilisation of DFB laser devices in microwave photonic signal processing is that they are coherent, i.e. they have narrow linewidth. Optical linewidth refers to the optical phase fluctuation of the lasing longitudinal modes. The need to minimise the effects of chromatic dispersion in optical fibres in long-haul telecommunication systems has been the main driving force behind the development of DFB laser devices having narrow linewidth.

Unlike telecommunication applications, photonic processing of microwave signals based on differential delays requires an incoherent optical carrier. To be absolutely accurate, the coherence time of the optical carrier must be shorter than the shortest differential delay in the photonic signal processor. Therefore, in order to utilise DFB laser devices in microwave photonic signal processing, their linewidth has to be broadened to reduce their coherence. Commercial DFB lasers have a typical linewidth of 1-10 MHz, which must be broadened to ~1 GHz for photonic processing, based on differential delays, to be applicable in EW systems operating at intermediate frequencies in the order of hundreds of MHz. Broadening linewidth of DFB laser devices is therefore the main focus of this report.

The investigation presented in this report is comprised of two parts. The first part focuses on the measurements of linewidth in single-mode DFB and multi-mode Fabry-Perot (FP) semiconductor lasers. The measurement was also extended to a wavelength-division multiplexed signal from a DFB device and a tunable laser source. The conclusion derived from these measurements clearly shows that the linewidth of multi-wavelength optical signals is not determined by the spectral spread of the lasing wavelengths. The overall linewidth distribution is a linear contribution of the phase fluctuations of each lasing wavelength. Therefore, FP laser devices can be coherent or incoherent, and their coherence does not depend on the spectral width because it is dominated by phase fluctuations of the longitudinal modes. Figure A on the next page illustrates the difference between the above-mentioned concepts of linewidth and spectral width.

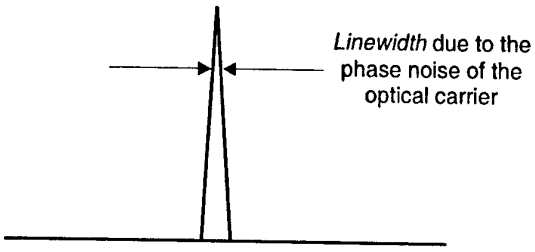

(i) Linewidth of a single-wavelength laser diode.

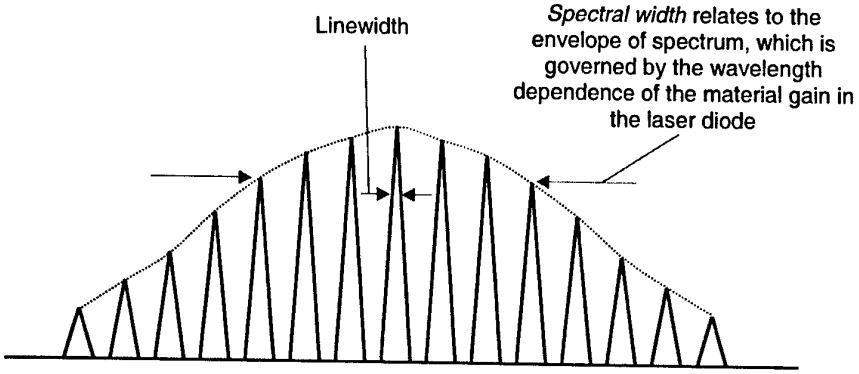

(ii) Linewidth and spectral width of a multiple-wavelength laser diode.

Figure A: Illustration of linewidth and spectral width.

The second part of the investigation focuses on a technique to broaden the linewidth of DFB lasers. A technique based on a simple combination of injection dithering and external phase modulation was able to broaden the linewidth of a DFB laser device from 10 MHz to over 200 MHz, while maintaining a continuous-wave (CW) optical carrier suitable for microwave photonic signal processing. This corresponds to a reduction of laser coherence length from 20 metres to less than 1 metre in optical fibres.

The work on laser coherence and a technique to broaden DFB laser linewidth represented in this report makes it possible for DFB semiconductor lasers to be used in microwave photonic signal processing. These commercial-off-the shelf (COTS) DFB devices can therefore be utilised as alternative sources to high-power FP devices in the development of photonic EW applications. In comparison to FP devices, DFB laser diodes are more readily available because of applications in telecommunications. The linewidth broadening technique presented in this report can also be applicable to compact tunable laser sources, which are currently competing to replace fixed-wavelength DFB lasers in telecommunications networking.

Author

Linh V T Nguyen
Electronic Warfare & Radar Division

Linh Nguyen received the BSc in 1992 and BE (EEE) in 1993 from the University of Adelaide, and PhD in 1997 from the Photonics Research Laboratory, Australian Photonics Cooperative Research Centre, Department of Electrical & Electronic Engineering, University of Melbourne.

He has held positions at the Photonics Research Laboratory, Vicom Australia Pty. Limited and Acterna Asia-Pacific Pty. Limited. He has also completed a Master of Marketing at the Melbourne Business School. He currently holds a Research Scientist position in the Electronic Warfare & Radar Division, DSTO Edinburgh, where his research interests are in the field of microwave photonic signal processing and its applications to Electronic Warfare. He is the Task Manager for Photonic Systems Technology in the Electronic Warfare & Radar Division.

Contents

1. Introduction

Microwave photonic signal processing in Electronic Warfare (EW) systems utilises the unique properties of optical fibres, such as low attenuation, wide bandwidth and immunity to electrical interference, to manipulate wideband radio frequency (RF), microwave and millimetre-wave signals [1]. Microwave photonic signal processors have been developed based on the theory and principles of digital filtering [2], where the digital differential delays are replaced with true-time optical differential delay techniques [3-9].

In order for the microwave signals to be combined coherently, the optical carrier has to be incoherent so as to avoid optical coherent interference. The optical coherence length has to be shorter than the smallest true-time differential delay implemented in the microwave photonic signal processor. For example, a distributed-feedback (DFB) semiconductor laser having a coherence length of 20 metres can only be used to process signals with frequencies less than 10 MHz [10-12]. However, EW systems often operate at frequencies ranging from hundreds of MHz to GHz, which makes DFB laser devices incompatible as sources for such microwave photonic signal processing applications, where high-frequency input signals are combined coherently.

The main driving force behind the development of highly coherent DFB laser devices has been to minimise the effects of chromatic dispersion in optical fibres in long-haul telecommunication transmission systems, which require DFB laser devices with the narrowest linewidth possible. However, DFB semiconductor lasers are attractive for deployment in microwave photonic signal processing due to their low cost and the applicability of dense wavelength-division multiplexing techniques [5]. In order to use these DFB lasers in microwave photonic signal processing, their coherence has to be reduced, i.e. linewidth broadened. The choice of using lasers in microwave photonic signal processing is dictated by performance concerning signal power and noise. There are incoherent sources such as light-emitting diodes (LEDs) and broadband sources based on erbium-doped fibres, but these optical sources do not deliver the performance required by EW applications.

It can be a mistake to believe that multi-mode Fabry-Perot (FP) semiconductor lasers are less coherent than single-mode DFB laser devices because of their wide spectral width. Such mistakes exist because the spectral width is often used interchangeably to represent both DFB linewidth and the width of the multi-mode optical spectrum [11]. For example, a FP laser device can manifest a linewidth of 30 MHz, while its -3 dB spectral width can be in the order of hundreds of GHz [13]. This implies that FP semiconductor lasers cannot be assumed to be incoherent when utilising them in microwave photonic signal processing without careful linewidth consideration.

The linewidth of DFB lasers can be simply broadened by direct small-signal modulation or injection dithering [10]. This is optical frequency modulation. Varying

the carrier population inside the active region of the laser device under direct modulation modifies the refractive index [10,14], thereby producing wavelength chirping due to the linewidth enhancement factor [14]. While such simple methods allow the linewidth of DFB lasers to be broadened, the direct modulation in turn affects their operational characteristics in addition to the modulation on the output optical carriers. The aim is to develop a simple technique to perform DFB linewidth broadening while maintaining continuous-wave (CW) optical carriers for microwave photonic signal processing. The research presented in this report utilises injection dithering and phase modulation to broaden the DFB linewidth.

During the process of completing this report, published research by Hotate and colleagues on the synthesis of optical coherence function for sensor applications [15-19] was brought to the author's attention. The author wishes to provide a comparison below to aid the readers in their understanding of the two applications:

Linewidth Broadening for Microwave Photonic Signal Processing	**Synthesis of Optical Coherence Function for Sensor Applications**
Injection dithering, i.e. small-signal direct modulation, to broaden the power spectrum while maintaining CW optical output. Of course, there is a small-signal modulation on the optical carrier. The linewidth is broadened without splitting the distribution into multiple peaks.	Large-signal direct modulation is required to generate a power spectrum with a pair of peaks, sometimes referred to as "rabbit-ears" [10]. This would require a large differential carrier population and so the optical output would be pulsed [10]. This is typically in sensor applications. In References 16 and 17, a tunable laser diode was used.
Phase modulation of the optical output at low electrical modulation frequency to enhance optical phase noise. The purpose of phase modulation is to overlap the replicated linewidth distributions, after injection dithering, effectively creating an optical carrier with a broader linewidth distribution. No synchronisation is required between the injection dithering and phase modulation.	Synchronous phase modulation is used in a reference arm of a Mach-Zehnder interferometer to generate the desired optical coherence function. The electrical modulation frequency is proportional to the optical modulated frequency achieved from direct modulation. The role of phase modulation in this application is to modify the optical differential delay time of the interferometer.
Linewidth is defined by the measured distribution of the optical phase noise using a phase-modulated self-heterodyning technique [20].	The optical coherence function is defined by the visibility of the interference pattern of the interferometer, which is a function of the differential delay time.

Hotate and colleagues [15-19] defined the optical coherence function as the Fourier transformation of the power spectrum of the light source, which is the linewidth distribution. From the work by Hotate and colleagues [15-19], if only the optical path from the laser diode through to the reference arm of the interferometer is considered, then it is similar to the work investigated by the author. However, the complete Mach-Zehnder interferometer must be considered as described in the next paragraph.

In simple terms, Hotate and colleagues started with a light source with very large linewidth [15-19]. This is achieved by frequency modulation with large-signal direct modulation or optical frequency tuning. Synchronous phase modulation selectively modifies the optical differential delay time of the interferometer causing constructive and destructive interference at desired offset frequencies [15-19]. Effectively, the interferometer acts as a tunable optical notch filter, which samples the broad linewidth distribution into discrete frequencies. This is how any arbitrary optical coherence function could be synthesised based on Fourier transformation [15-19]. However, this sampled linewidth distribution would no longer be suitable for microwave photonic signal processing. In addition to the large-signal modulation on the optical carrier, the sampled linewidth is effectively a multiplexed signal made up of many signals that have small linewidth distributions, defeating the purpose of linewidth broadening.

The research presented in this report is not so much about the synthesis of linewidth distribution or optical coherence function, but it simply focuses on the broadening of DFB linewidth for microwave photonic signal processing. The structure of this report is arranged into the following sections:

- *Optical Linewidth Measurement Techniques* section outlines the preferred method to measure linewidth of semiconductor lasers.
- *Linewidth of Multi-Wavelength Optical Carriers* section presents measurements of linewidth of a wavelength-division multiplexed signal and a FP laser device to study any dependency on the spectral distribution.
- *Linewidth of Phase-Modulated Optical Carriers* section presents measurements of external phase modulation as an initial step to investigate techniques to broaden the linewidth of DFB semiconductor lasers.
- *Linewidth Broadening of DFB Lasers* section presents the results of linewidth broadening based on a combination of injection dithering and external phase modulation. Discussion on its limitation will be addressed.
- *Conclusions* summarise the findings of this report.
- *Recommendations* detail the application of DFB laser devices in microwave photonic signal processing and future research directions.

2. Optical Linewidth Measurement Techniques

In this section, analysis of techniques to measure linewidth of semiconductor lasers will be presented. The techniques to be analysed are based on delayed self-heterodyning of the optical carrier.

2.1 Delayed Self-Heterodyning Method

Delayed self-heterodyning is known to be among the most sensitive method to analyse laser linewidth [20]. Such an interferometric arrangement is shown in Figure 1.

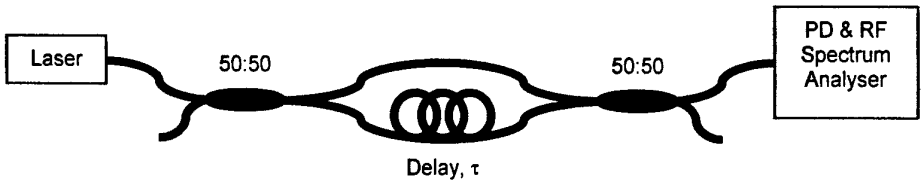

Figure 1: Delayed self-heterodyning interferometric arrangement.

The analysis of linewidth distribution based on delayed self-heterodyning represented in this report will follow that of Reference 20. For simplicity, the coupling coefficients of the optical couplers can be ignored in the analysis of the interferometer without losing its generality. The input optical fields of the upper and lower arms of the interferometer, respectively, are:

$$\overrightarrow{E_{up}(t)} = E_o e^{j(\omega_o t+\varphi(t))} \tag{1}$$

$$\overrightarrow{E_{lo}(t)} = \overrightarrow{E_{up}(t)} = E_o e^{j(\omega_o t+\varphi(t))} \tag{2}$$

where E_o is the optical field amplitude, ω_o and $\varphi(t)$ are optical frequency and phase fluctuation function, respectively.

At the photodetector, which is assumed to have unity responsivity, the current produced is given as:

$$I(t,\tau) = \left(\overrightarrow{E_{up}(t)} + \overrightarrow{E_{lo}(t+\tau)}\right)\left(\overrightarrow{E_{up}(t)} + \overrightarrow{E_{lo}(t+\tau)}\right)^* \tag{3}$$

$$\begin{aligned} I(t,\tau) = &\left(E_o e^{j(\omega_o t+\varphi(t))} + E_o e^{j(\omega_o (t+\tau)+\varphi(t+\tau))}\right) \times \\ &\left(E_o e^{-j(\omega_o t+\varphi(t))} + E_o e^{-j(\omega_o (t+\tau)+\varphi(t+\tau))}\right) \end{aligned} \tag{4}$$

Expanding and simplifying the various terms give:

$$\begin{aligned} I(t,\tau) &= 2E_o^2 + E_o^2 e^{j(\varphi(t)-\omega_o\tau-\varphi(t+\tau))} + E_o^2 e^{-j(\varphi(t)-\omega_o\tau-\varphi(t+\tau))} \\ &= 2E_o^2\{1+\cos(\varphi(t)-\omega_o\tau-\varphi(t+\tau))\} \end{aligned} \quad (5)$$

Provided that the delay, τ, is much longer than the coherence length of the laser, it can be shown that the electrical spectral density of the current consists of a DC term and a Lorentzian distribution centred at DC [20]. The Lorentzian distribution is a result of the phase fluctuation, $\varphi(t)-\varphi(t+\tau)$. Interested readers can refer to Reference 20 for a full analysis of the temporal coherence function and its spectral density. The full width at half maximum of the Lorentzian distribution gives a measurement of the linewidth, $\Delta\upsilon$, of the optical input carrier [20]. However, there are two problems in determining the linewidth using this interferometric arrangement:

1. The Lorentzian distribution is centred at DC, where there is a large DC component.
2. Commercial wideband spectrum analysers do not operate near DC.

In order to take an accurate linewidth measurement, the Lorentzian linewidth distribution must be shifted away from DC. This is achieved by using an optical phase modulator in the upper arm of interferometric arrangement shown in Figure 1.

2.2 Phase-Modulated Delayed Self-Heterodyning Method

The phase-modulated delayed self-heterodyning interferometric arrangement is shown in Figure 2. This arrangement is the same as Figure 1, apart from the addition of an optical phase modulator (PM) on the upper arm. It is assumed that the phase noise of the electrical signal, Ω_{RF}, is low and has negligible effect on the laser linewidth.

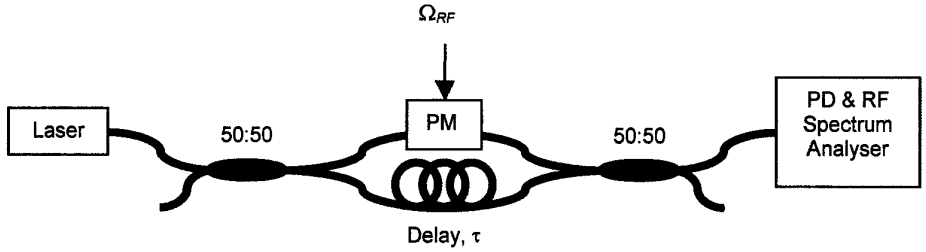

Figure 2: Phase-modulated delayed self-heterodyning interferometric arrangement.

The analysis starts out similarly with Equations 1 and 2. At the output of the optical phase modulator, having a modulating index, δ, and fibre delay, the optical fields are:

$$\overrightarrow{E_{PM}(t)} = E_o e^{j(\omega_o t+\varphi(t)+\delta\sin(\Omega_{RF}t))} \quad (6)$$

$$\overline{E_{Delay}(t+\tau)} = E_o e^{j(\omega_o(t+\tau)+\varphi(t+\tau))} \tag{7}$$

The current produced by the detector is:

$$I(t,\tau) = \left(\overline{E_{PM}(t)} + \overline{E_{Delay}(t+\tau)}\right)\left(\overline{E_{PM}(t)} + \overline{E_{Delay}(t+\tau)}\right)^* \tag{8}$$

$$I(t,\tau) = \left(E_o e^{j(\omega_o t+\varphi(t)+\delta\sin(\Omega_{RF}t))} + E_o e^{j(\omega_o(t+\tau)+\varphi(t+\tau))}\right) \times \left(E_o e^{-j(\omega_o t+\varphi(t)+\delta\sin(\Omega_{RF}t))} + E_o e^{-j(\omega_o(t+\tau)+\varphi(t+\tau))}\right) \tag{9}$$

Expanding and simplifying the various terms give:

$$I(t,\tau) = 2E_o^2 + E_o^2 e^{j(\varphi(t)-\omega_o\tau-\varphi(t+\tau))} e^{j\delta\sin(\Omega_{RF}t)} + E_o^2 e^{-j(\varphi(t)-\omega_o\tau-\varphi(t+\tau))} e^{-j\delta\sin(\Omega_{RF}t)} \tag{10}$$

Using the following trigonometric relation:

$$-\sin(x) = \sin(-x) \tag{11}$$

The current can then be rewritten as:

$$I(t,\tau) = 2E_o^2 + E_o^2 e^{j(\varphi(t)-\omega_o\tau-\varphi(t+\tau))} e^{j\delta\sin(\Omega_{RF}t)} + E_o^2 e^{-j(\varphi(t)-\omega_o\tau-\varphi(t+\tau))} e^{j\delta\sin(-\Omega_{RF}t)} \tag{12}$$

Utilising the following transformation with Bessel functions [21]:

$$e^{j\delta\sin y} = \sum_{m=-\infty}^{\infty} J_m(\delta) e^{jmy}$$
$$J_{-m}(\delta) = (-1)^m J_m(\delta) \tag{13}$$

Examples of Bessel functions of orders 0 to 5 are plotted in Figure 3. This is included so that readers can compare the measured responses of a particular phase modulator, described in a later section. Substituting Equation 13 into 12 gives:

$$I(t,\tau) = 2E_o^2 + E_o^2 e^{j(\varphi(t)-\omega_o\tau-\varphi(t+\tau))} \sum_{m=-\infty}^{\infty} J_m(\delta) e^{jm\Omega_{RF}t} + E_o^2 e^{-j(\varphi(t)-\omega_o\tau-\varphi(t+\tau))} \sum_{m=-\infty}^{\infty} J_m(\delta) e^{-jm\Omega_{RF}t} \tag{14}$$

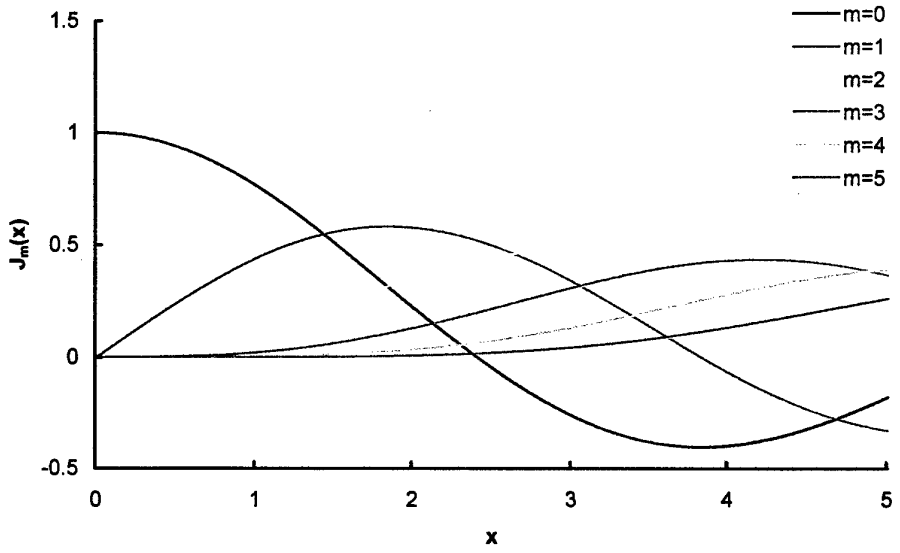

Figure 3: Examples of Bessel functions of orders 0 to 5.

Rearranging Equation 14 results in the following:

$$I(t,\tau) = 2E_o^2 + E_o^2 \sum_{m=-\infty}^{\infty} J_m(\delta)\, e^{j(\varphi(t)-\omega_o\tau-\varphi(t+\tau)+m\Omega_{RF}t)} + E_o^2 \sum_{m=-\infty}^{\infty} J_m(\delta) e^{-j(\varphi(t)-\omega_o\tau-\varphi(t+\tau)+m\Omega_{RF}t)} \quad (15)$$
$$= 2E_o^2\left\{1+\sum_{m=-\infty}^{\infty} J_m(\delta)\cos(\varphi(t)-\omega_o\tau-\varphi(t+\tau)+m\Omega_{RF}t)\right\}$$

Equation 15 is in a similar form to Equation 5. By comparing Equations 5 and 15, it can be seen that the electrical spectral density of the current in Equation 15 consists of a DC term and Lorentzian linewidth distribution centred at $m\Omega_{RF}$ for integer $0 \le m < \infty$, when only positive frequencies are considered. The strength of the Lorentzian linewidth distribution centred at $m\Omega_{RF}$ will be determined by $|J_m(\delta)|$. The negative sign from the Bessel functions (Equation 13 and Figure 3) is absorbed by the cosine function, i.e. $-\cos(x) = \cos(\pi - x)$. It is sufficient to study the linewidth distribution at $m = 1$. This is true when δ is small, where $J_0(\delta)$ and $J_1(\delta)$ terms are dominant as shown in Figure 3. Once again, the delay, τ, must be much longer than the coherence length of the laser. A fibre delay of around 5 km is generally more than adequate. This method of using an optical phase modulator in the delayed self-heterodyning

interferometric arrangement replicates the optical linewidth distribution at Ω_{RF} to first-order approximation, which overcomes the problems associated with using commercial wideband spectrum analysers. The actual configuration of the phase-modulated delayed self-heterodyning interferometer, which was used to perform all linewidth measurements in this work, is as shown in Figure 4.

Throughout the analysis depicted in Equations 1-15 and the self-heterodyning interferometer shown in Figure 4, an ideal 3 dB (i.e. 50:50) optical coupler has been assumed. A similar analysis can be generalised for an uneven coupling ratio. The consequence of a small deviation from the ideal coupling ratio, say 51:49, found in commercial 3 dB optical couplers would be negligible.

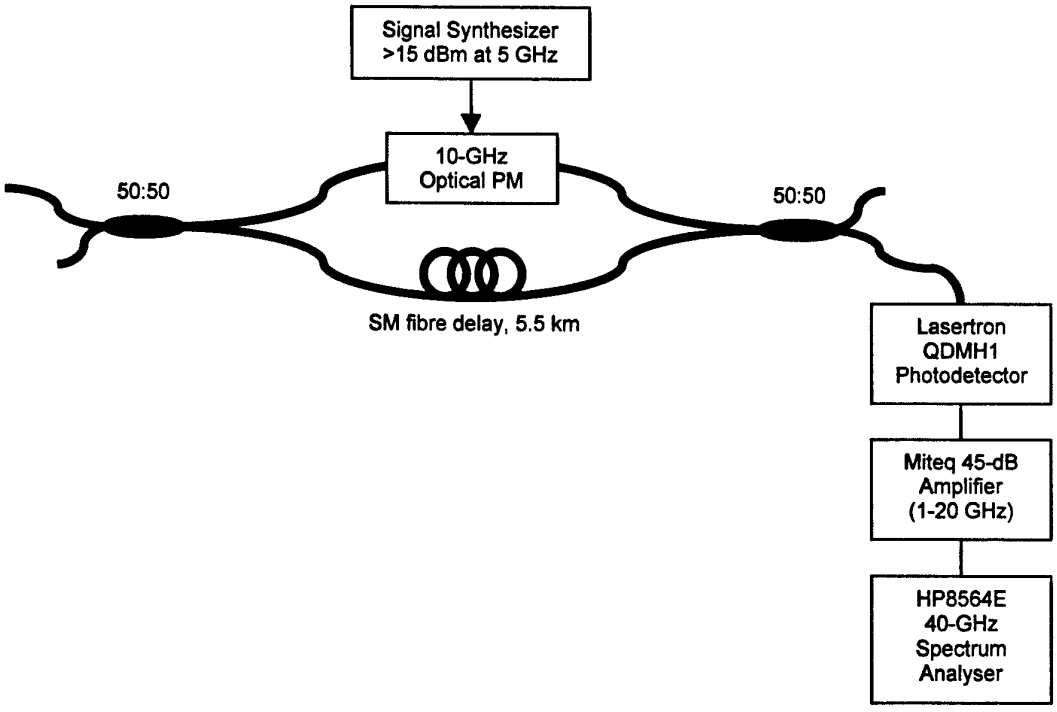

Figure 4: Actual configuration of the phase-modulated delayed self-heterodyning interferometer used to perform all linewidth measurements.

2.3 Laser Linewidth and Coherence Length

The coherence length of a laser is related to its linewidth by the following [12]:

$$l_c = \frac{c}{\pi n_g \Delta\upsilon} \tag{16}$$

where c is the speed of light in vacuum, n_g is the group index of refraction of the propagation medium, and $\Delta\upsilon$ is the linewidth.

Although Equation 16 is the actual coherence length, it is common in optoelectronics to use the expression:

$$l_c = \frac{c}{n_g \Delta\upsilon} \tag{17}$$

For ease of comparison with other works, Equation 17 is used to determine laser coherence length throughout this report.

3. Linewidth of Multi-Wavelength Optical Carriers

It is often believed that Fabry-Perot (FP) semiconductor lasers are incoherent optical sources because of the broad spectral width, as compared to distributed-feedback (DFB) laser devices. In this section, analysis and measurements are presented to investigate any dependency of linewidth of multi-wavelength optical carriers on spectral distribution.

3.1 Theoretical Analysis

The analysis of multiple-wavelength optical carriers presented here is similar to that of the phase-modulated delayed self-heterodyning method in the last section. However, the analysis is generalised to N wavelengths. The author could not locate the analysis presented below in the open literature. The inputs to the upper and lower arms of the interferometer are:

$$\overrightarrow{E_{up}(t)} = \sum_{k=1}^{N} E_k e^{j(\omega_k t + \varphi_k(t))} \tag{18}$$

$$\overrightarrow{E_{lo}(t)} = \overrightarrow{E_{up}(t)} = \sum_{k=1}^{N} E_k e^{j(\omega_k t + \varphi_k(t))} \tag{19}$$

The fields at the outputs of the phase modulator and fibre delay are:

$$\overrightarrow{E_{PM}(t)} = \sum_{k=1}^{N} E_k e^{j(\omega_k t + \varphi_k(t) + \delta \sin(\Omega_{RF} t))} \tag{20}$$

$$\overrightarrow{E_{Delay}(t+\tau)} = \sum_{k=1}^{N} E_k e^{j(\omega_k (t+\tau_k) + \varphi_k(t+\tau_k))} \tag{21}$$

where τ is average delay in the interferometer and τ_k accounts for the dependence on wavelength in a dispersive delay medium. Combining the signals at the photodetector gives the following current:

$$I(t,\tau) = \left(\overrightarrow{E_{PM}(t)} + \overrightarrow{E_{Delay}(t+\tau)}\right)\left(\overrightarrow{E_{PM}(t)} + \overrightarrow{E_{Delay}(t+\tau)}\right)^{*} \tag{22}$$

$$I(t,\tau)=\left(\sum_{k=1}^{N}E_k e^{j(\omega_k t+\varphi_k(t)+\delta\sin(\Omega_{RF}t))}+\sum_{k=1}^{N}E_k e^{j(\omega_k(t+\tau_k)+\varphi_k(t+\tau_k))}\right)\times \left(\sum_{k=1}^{N}E_k e^{-j(\omega_k t+\varphi_k(t)+\delta\sin(\Omega_{RF}t))}+\sum_{k=1}^{N}E_k e^{-j(\omega_k(t+\tau_k)+\varphi_k(t+\tau_k))}\right) \quad (23)$$

Expanding the brackets gives:

$$\begin{aligned}I(t,\tau)=&\sum_{k=1}^{N}E_k e^{j(\omega_k t+\varphi_k(t)+\delta\sin(\Omega_{RF}t))}\sum_{k=1}^{N}E_k e^{-j(\omega_k t+\varphi_k(t)+\delta\sin(\Omega_{RF}t))}+\\ &\sum_{k=1}^{N}E_k e^{j(\omega_k t+\varphi_k(t)+\delta\sin(\Omega_{RF}t))}\sum_{k=1}^{N}E_k e^{-j(\omega_k(t+\tau_k)+\varphi_k(t+\tau_k))}+\\ &\sum_{k=1}^{N}E_k e^{j(\omega_k(t+\tau_k)+\varphi_k(t+\tau_k))}\sum_{k=1}^{N}E_k e^{-j(\omega_k t+\varphi_k(t)+\delta\sin(\Omega_{RF}t))}+\\ &\sum_{k=1}^{N}E_k e^{j(\omega_k(t+\tau_k)+\varphi_k(t+\tau_k))}\sum_{k=1}^{N}E_k e^{-j(\omega_k(t+\tau_k)+\varphi_k(t+\tau_k))}\end{aligned} \quad (24)$$

Expanding the wavelengths gives:

$$\begin{aligned}I(t,\tau)=&\sum_{k=1}^{N}E_k^2+\sum_{k=1,l=1,k\neq l}^{N}E_k E_l e^{j((\omega_k-\omega_l)t+\varphi_k(t)-\varphi_l(t))}+\\ &\sum_{k=1}^{N}E_k^2 e^{j(\varphi_k(t)-\omega_k\tau_k-\varphi_k(t+\tau_k)+\delta\sin(\Omega_{RF}t))}+\\ &\sum_{k=1,l=1,k\neq l}^{N}E_k E_l e^{j((\omega_k-\omega_l)t+\varphi_k(t)-\omega_l\tau_l-\varphi_l(t+\tau_l)+\delta\sin(\Omega_{RF}t))}+\\ &\sum_{k=1}^{N}E_k^2 e^{-j(\varphi_k(t)-\omega_k\tau_k-\varphi_k(t+\tau_k)+\delta\sin(\Omega_{RF}t))}+\\ &\sum_{k=1,l=1,k\neq l}^{N}E_k E_l e^{-j((\omega_k-\omega_l)t+\varphi_k(t)-\omega_l\tau_l-\varphi_l(t+\tau_l)+\delta\sin(\Omega_{RF}t))}+\\ &\sum_{k=1}^{N}E_k^2+\sum_{k=1,l=1,k\neq l}^{N}E_k E_l e^{j((\omega_k-\omega_l)t+\omega_k\tau_k-\omega_l\tau_l+\varphi_k(t+\tau_k)-\varphi_l(t+\tau_l))}\end{aligned} \quad (25)$$

Equation 25 is a combination of the beat signals of different wavelengths, $e^{j(\omega_k-\omega_l)t}$, and the linewidth distributions. If all of the beat signals are ignored, i.e. assuming that the smallest beat frequency is higher than the bandwidth of the photodetector, then the current is reduced to:

$$I(t,\tau)=\sum_{k=1}^{N}E_k^2+\sum_{k=1}^{N}E_k^2e^{j(\varphi_k(t)-\omega_k\tau_k-\varphi_k(t+\tau_k)+\delta\sin(\Omega_{RF}t))}+\sum_{k=1}^{N}E_k^2e^{-j(\varphi_k(t)-\omega_k\tau_k-\varphi_k(t+\tau_k)+\delta\sin(\Omega_{RF}t))}+\sum_{k=1}^{N}E_k^2 \tag{26}$$

$$I(t,\tau)=\sum_{k=1}^{N}\left(2E_k^2+E_k^2e^{j(\varphi_k(t)-\omega_k\tau_k-\varphi_k(t+\tau_k)+\delta\sin(\Omega_{RF}t))}+E_k^2e^{-j(\varphi_k(t)-\omega_k\tau_k-\varphi_k(t+\tau_k)+\delta\sin(\Omega_{RF}t))}\right) \tag{27}$$

This is in the same form as Equation 10. It states that the electrical spectral density of the current produced is a summation of the self-heterodyning spectrum of each wavelength. Therefore, the linewidth distribution of a wavelength-division multiplexed optical signal does not depend on the wavelength distribution or spacing. This is a very interesting finding from the analysis presented, which may seem to be self-evident and trivial to laser physicists, but it is important to the understanding of coherence in FP laser devices in microwave photonic signal processing. The overall coherence in FP laser devices is determined by the contributions of each longitudinal mode, and not by the broad spectral width. The spectral width may have its own coherence, but the laser coherence is dominated by the contributions of the longitudinal modes.

3.2 Linewidth of a Fabry-Perot Laser

To verify the theoretical result in Equation 27, the linewidth of a FP laser device was measured. The experiment was set up as shown in Figure 5. The laser device is a Mitsubishi FU-624SHL-4 biased at 40 mA. An E-tek optical isolator was needed to minimise back-reflection into the laser affecting its true unbroadened linewidth. The optical bandpass filter (BPF) is a Dicon TF-9-1565-1-FC-P-0.9. An optical spectrum analyser (OSA — Anritsu MS9710B) was also used.

The BPF was used to investigate if the broad spectral width of the FP laser device influences the linewidth measurement. The unfiltered and filtered optical spectra of the laser are shown in Figure 6. The BPF was tuned to the peak of the laser spectrum. The respective linewidth distributions of the unfiltered and filtered outputs of FU-624SHL-4 are as depicted in Figure 7. The weak modulation was due to the residual back-reflection. The laser was operating in the coherence collapse regime [13] when there was no isolator, i.e. the linewidth was broadened beyond detection (below the

floor). The peak of the linewidth distribution for both unfiltered and filtered outputs are similar. Optical filtering attenuated the strength of the linewidth distribution in Figure 7(b), but did not affect the shape of the distribution. The coherence is still dominated by the contributions of the filtered longitudinal modes. The attenuation is related to the weaker strength of filtered longitudinal modes. This is the first part of the experimental confirmation of the theoretical expression in Equation 27.

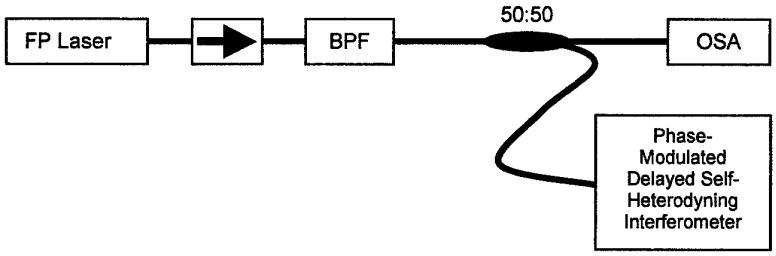

Figure 5: Arrangement to measure linewidth of a FP laser.

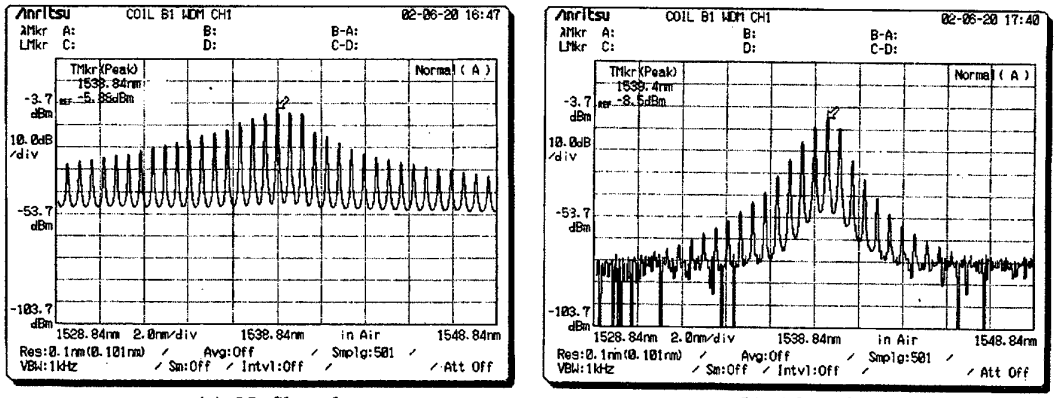

(a) Unfiltered *(b) Filtered*

Figure 6: Unfiltered and filtered optical spectra of FU-624SHL-4 biased at 40 mA.

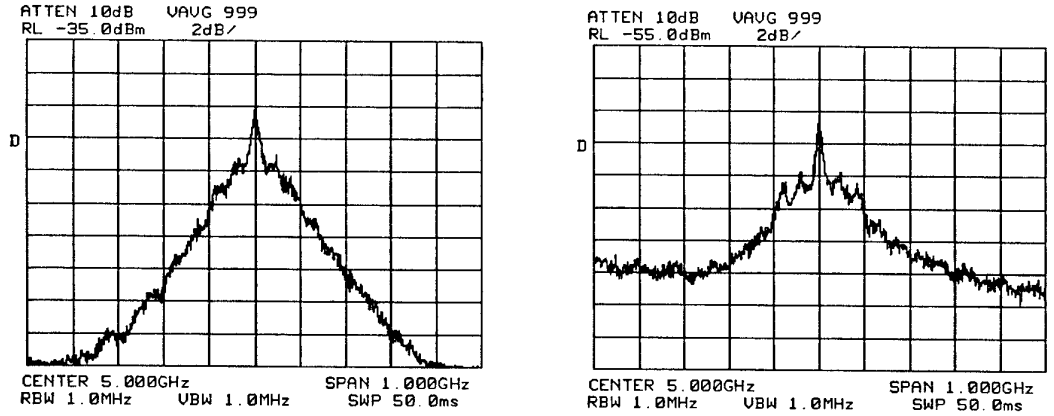

(a) Unfiltered *(b) Filtered*

Figure 7: Linewidth distribution of unfiltered and filtered outputs. Weak spectral modulation due to residual back-reflection makes it difficult to estimate the FP laser linewidth.

From Equation 27 and Figure 6(a), one may be mistaken to assume that all the longitudinal modes in a FP laser device would have the same Lorentzian linewidth distribution. This is not necessarily true because semiconductor laser phase noise, and hence linewidth, is dependent on the differential refractive index and gain [14]. Both of these parameters are dependent on wavelength [10,14]. Furthermore, the modal linewidth in Figure 6(a) is misleading due to the dispersive characteristics of the OSA.

3.3 Linewidth of a Wavelength-Division Multiplexed Signal

In order to consolidate the experimental confirmation of Equation 27, linewidth measurements were carried out with a two-wavelength multiplexed optical carrier. The experiment was set up as depicted in Figure 8. A distributed-feedback (DFB) laser diode (Alcatel A 1905 LMI) and a tunable laser source (TLS — Anritsu MG9638A) were coupled together to form a two-wavelength multiplexed optical carrier. The TLS has a coherence control on-off function, which was useful in this investigation.

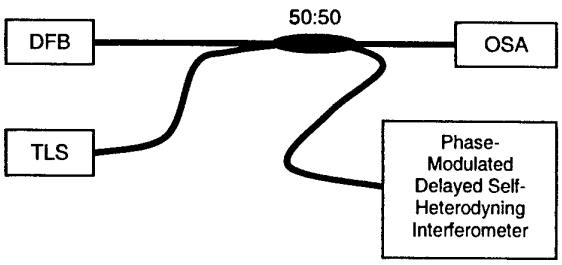

Figure 8: Linewidth measurement of a wavelength-division multiplexed optical carrier.

The optical spectrum of A 1905 LMI biased at 30 mA is shown in Figure 9(a). The laser operated near 1556 nm, and the side-mode suppression ratio was around 40 dB. The linewidth of the laser was measured to be around 2 MHz, which corresponds to a coherence length of 100 metres in optical fibres. The linewidth distribution is shown in Figure 9(b). Therefore, this DFB laser can only be used to coherently process radio-frequency (RF) signals of less that 2 MHz.

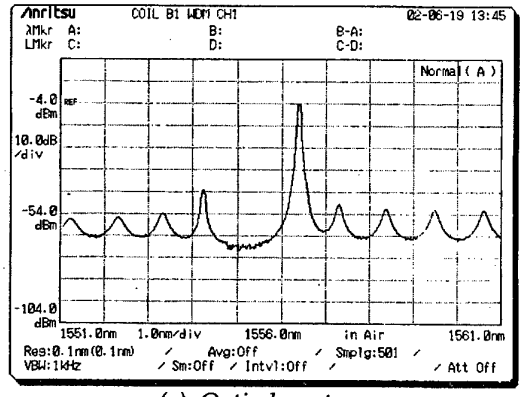

(a) Optical spectrum

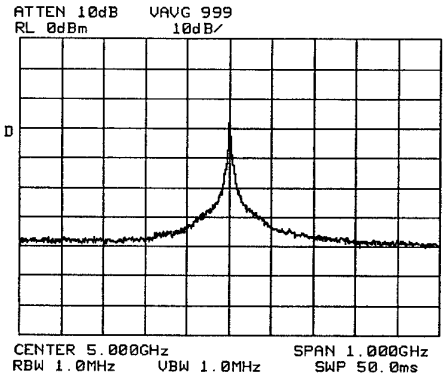

(b) Linewidth distribution

Figure 9: Optical spectrum and linewidth distribution of A 1905 LMI bias at 30 mA.

The optical spectra of the TLS are as shown in Figure 10 for both coherence controls off and on. The output power and wavelength were tuned to match the A 1905 LMI laser device, shown in Figure 9(a). There is no difference between the two optical spectra when coherence control is altered, because the OSA is a dispersive-grating based instrument and therefore it does not have MHz or sub-picometre resolution to measure laser linewidth. However, the linewidth distributions, shown in Figure 11, are significantly different. The linewidth measurements were 1 MHz and 100 MHz for coherence controls off and on, respectively, as appears in Figure 11.

A notch splits the linewidth distribution with coherence control on, depicted in Figure 11(b). This is a function of the proprietary linewidth broadening mechanism built into the laser by the manufacturer. This notch would effectively halve the linewidth of the laser to 50 MHz, as specified by the manufacturer.

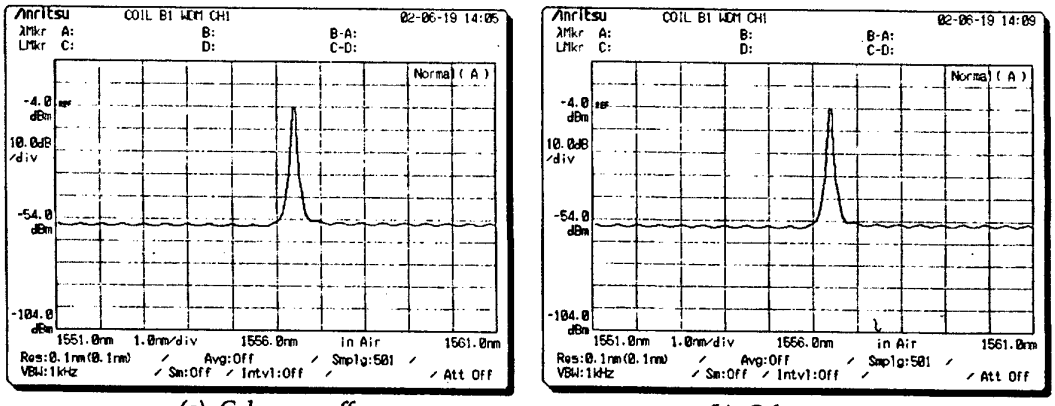

(a) Coherence off *(b) Coherence on*

Figure 10: Optical spectra of the TLS.

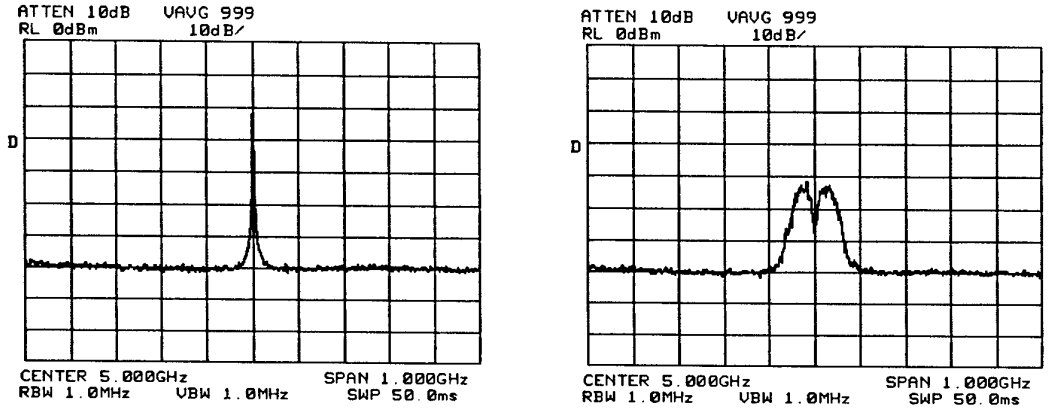

(a) Coherence off *(b) Coherence on*

Figure 11: Linewidth distribution of the TLS.

Figure 12 shows the optical spectra of the multiplexed outputs from the A 1905 LMI biased at 30 mA, shown in Figure 9(a), and the TLS tuned to 1556.68 nm, 1556.60 nm and 1556.00 nm, respectively. These wavelength readings are on the TLS, whereas the OSA has a small offset of around -0.3 nm compared to the TLS. These spectra were the same for both TLS coherence controls off and on. Figure 13 depicts the corresponding self-heterodyning spectra of the same multiplexed optical carriers shown in Figure 12. The TLS coherence control was off. The three cases are:

1. λ_{TLS} =1556.68 nm: There was a residual wavelength difference between A 1905 LMI and the TLS. The difference showed up as a 700 MHz beat signal on the self-heterodyning spectrum, shown in Figure 13(a), as predicted in Equation 25.
2. λ_{TLS} =1556.60 nm: The wavelength difference is 0.08 nm corresponding to 10 GHz, which is clearly identified on Figure 13(b). The optical spectrum, Figure 12(b),

shows what looks to be linewidth broadening due to grating dispersion, but the self-heterodyning spectrum in Figure 13(b) does not.

3. λ_{TLS} =1556.00 nm: Figure 13(c) simply shows the linewidth distribution without any beat signal because it was no longer within the detection bandwidth.

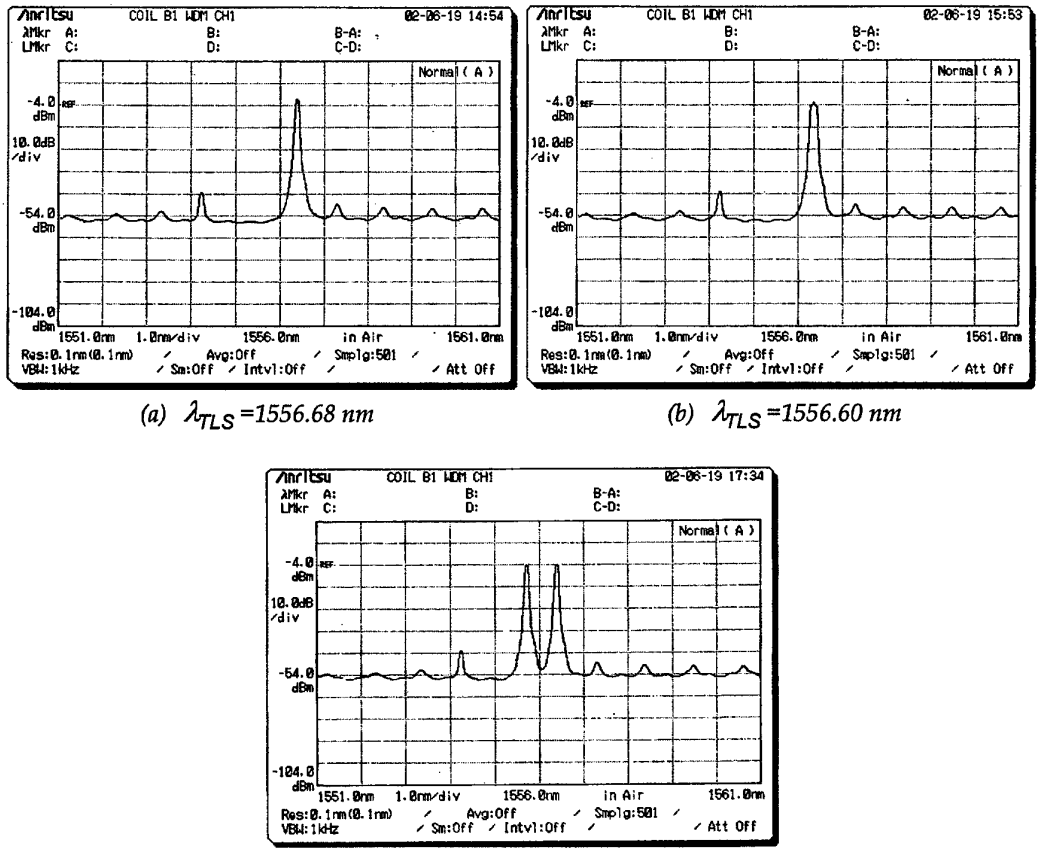

(a) λ_{TLS} *=1556.68 nm* *(b)* λ_{TLS} *=1556.60 nm*

(c) λ_{TLS} *=1556.00 nm*

Figure 12: Spectra of multiplexed outputs from A 1905 LMI and TLS.

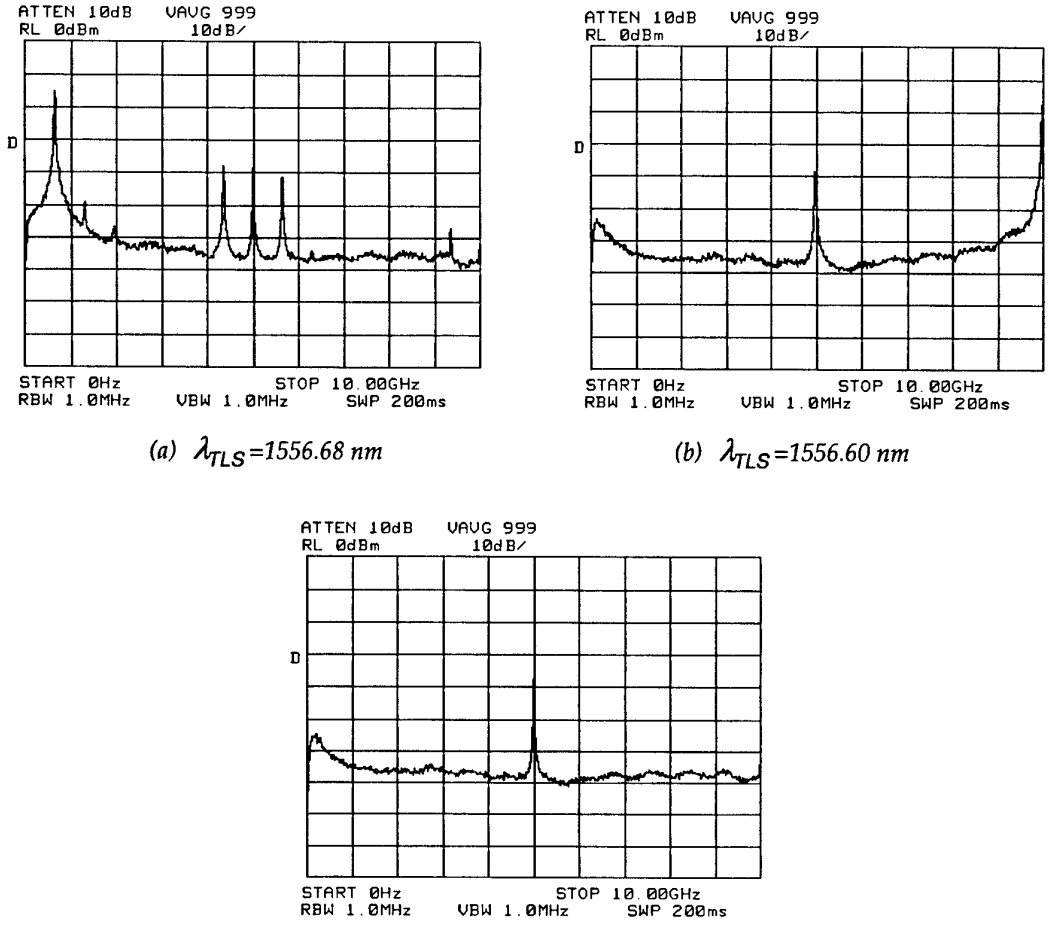

(a) λ_{TLS}*=1556.68 nm*

(b) λ_{TLS}*=1556.60 nm*

(c) λ_{TLS}*=1556.00 nm*

Figure 13: Self-heterodyning spectra of multiplexed outputs from A 1905 LMI and TLS.

Figure 13(c) cannot complete the experimental proof for Equation 27. The measurements needed to do so are shown in Figure 14. These are the linewidth measurements of the multiplexed output from the A 1905 LMI and TLS. The TLS was tuned to 1556.00 nm and its coherence controls were off and on, respectively. It is not so obvious on Figure 14(a), but Figure 14(b) clearly illustrates that the linewidth of the A 1905 LMI has filled in the notch of the linewidth distribution of the TLS. In addition, Figure 14 reinforces the finding in relation to the FP linewidth measurements presented earlier. In addition, Figure 14 is not an example of the synthesis of linewidth distribution. It is simply a part of the experimental verification of Equation 27.

The linewidth of the wavelength-division multiplexed optical carrier does not depend on the spectral distribution or wavelength spacing. This completes the experimental verification of Equation 27.

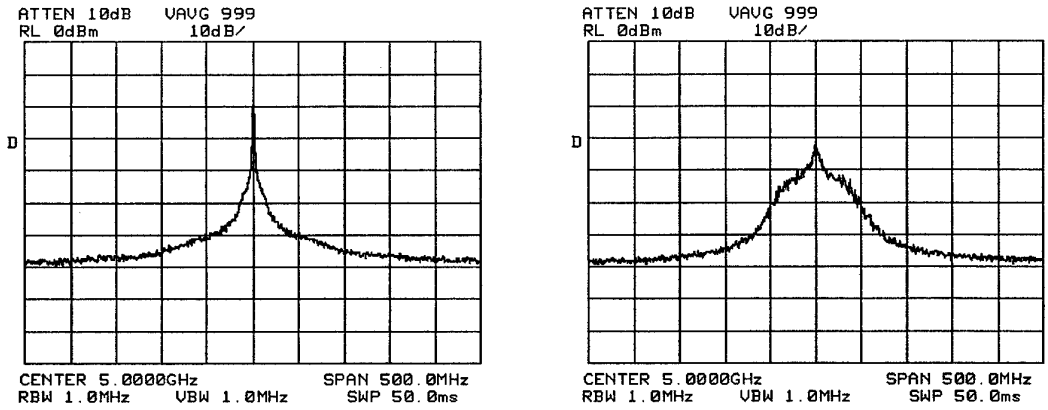

(a) Coherence off *(b) Coherence on*

Figure 14: Self-heterodyning spectra of multiplexed outputs from A 1905 LMI and TLS with λ_{TLS}=1556.00 nm.

3.4 Summary

The main finding of this section is that the linewidth of a multi-wavelength optical carrier does not depend on the spectral distribution or wavelength spacing. The resultant linewidth distribution is a linear combination of the contributions from each wavelength. This implies that FP laser devices can be coherent or incoherent, i.e. they can have both short or long coherence lengths, respectively. Their use in microwave photonic signal processing must be applied selectively.

The finding of this section is perhaps well known to laser physicists. However, it is presented in this research report for completeness. In addition, its emphasis in this report is to ensure that engineers, working in microwave photonic signal processing, appreciate the difference between linewidth and spectral width.

4. Linewidth of Phase-Modulated Optical Carriers

Essentially, internal phase modulation techniques to broaden laser linewidth are well known [10]. Linewidth broadening can be achieved internally by varying the refractive index in the active region with injection dithering [10]. Another technique is to vary the temperature of the active region, which then causes the emission wavelength to fluctuate [10].

The aim of the research is to experimentally analyse techniques to perform linewidth broadening externally without affecting the dynamics of the laser devices under operation. Components used in the various experiments are commercial-of-the-shelf (COTS). Phase modulation to synthesise optical coherence function is common in the area of low-coherence sensors [15-19,22]. In reference to microwave photonics, phase modulation has been reported in signal synthesis [23]. For completeness, external phase modulation is achieved with electro-optic material such as lithium niobate ($LiNbO_3$). This section reviews major points of the investigation into the use of an electro-optic phase modulator to broaden the DFB laser linewidth.

4.1 Phase-Modulated Optical Field

Recalling Equation 6, the phase-modulated optical field can be re-written as:

$$\overrightarrow{E_{PM}(t)} = E_o e^{j(\omega_o t+\varphi(t))} e^{j\delta \sin(\Omega_{RF} t)} \tag{28}$$

By using the transformation with Bessel function identity in Equation 13, the phase-modulated optical field becomes

$$\overrightarrow{E_{PM}(t)} = E_o e^{j(\omega_o t+\varphi(t))} \sum_{m=-\infty}^{\infty} J_m(\delta)\, e^{jm\Omega_{RF} t} \tag{29}$$

$$\overrightarrow{E_{PM}(t)} = E_o \sum_{m=-\infty}^{\infty} J_m(\delta)\, e^{j((\omega_o+m\Omega_{RF})t+\varphi(t))} \tag{30}$$

The optical spectral density of the phase-modulated optical field would have components at $\omega_o \pm m\Omega_{RF}$ for integer $m \geq 0$. The modulating index, δ, would determine the strength of each component according to the Bessel function, $J_m(\delta)$. An OSA based on dispersive optics, such as the Anritsu MS9710B, cannot resolve the spectral density of a phase-modulated optical carrier. A self-heterodyning interferometer is therefore required.

4.2 Characterising Phase Modulators

The voltage required to achieve π optical phase shift, V_π, provides little information on how the phase modulator behaves as a function of electrical input power and frequency. The phase modulator has to be characterised in reference to the electrical input parameters, such as power and frequency. The phase-modulated delayed self-heterodyning interferometer illustrated in Figure 4 was utilised to characterise phase modulators. The self-heterodyning spectrum shows the linewidth distribution being replicated at the electrical input frequency and its harmonics. An example is shown in Figure 15 illustrating such replication of the laser linewidth distribution over a large detection bandwidth.

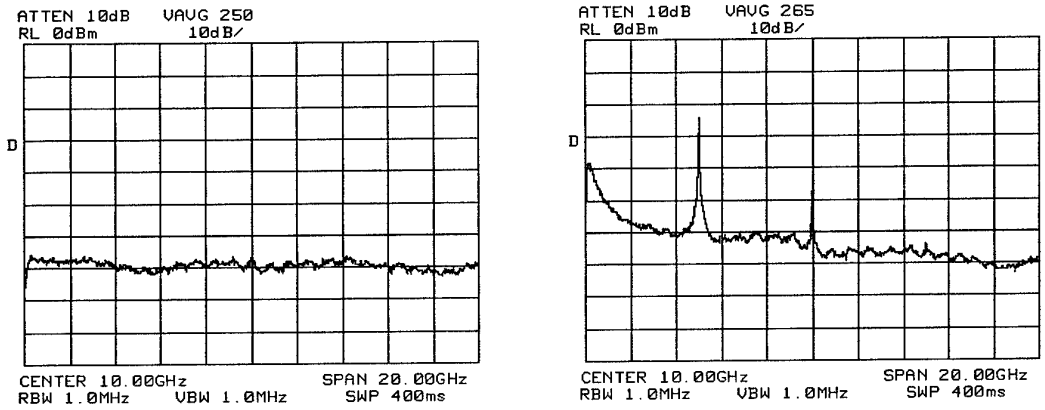

(a) No laser *(b) With A 1905 LMI*

Figure 15: Typical wideband self-heterodyning spectrum of A 1905 LMI showing harmonics of the replication of the linewidth distribution. In (b), Four peaks can be identified at DC, 5, 10 and 15 GHz. These corresponds to m=0, 1, 2 and 3 in Equation 15.

By adjusting the electrical input parameters and measuring the power of each linewidth replication above the noise floor, the results would then form the response of the phase modulator to the input. Figures 16 to 18 are the modulation responses of a JDS Uniphase PM150-000738 phase modulator, operating at 1550 nm with an electrical bandwidth of 10 GHz.

At the modulation frequencies of 2-10 GHz, the highest harmonic excited above the noise floor was third order, as shown in Figure 18. The harmonic excitation in phase modulator was more significant near 1 GHz with the sixth-order harmonic observed, as depicted Figure 19(a). However, only the third-order harmonic was observed at 500 MHz, as shown in Figure 19(b). This suggests harmonic excitation resonance around 1 GHz, which is inherent to this particular phase modulator and may not be general in all phase modulators.

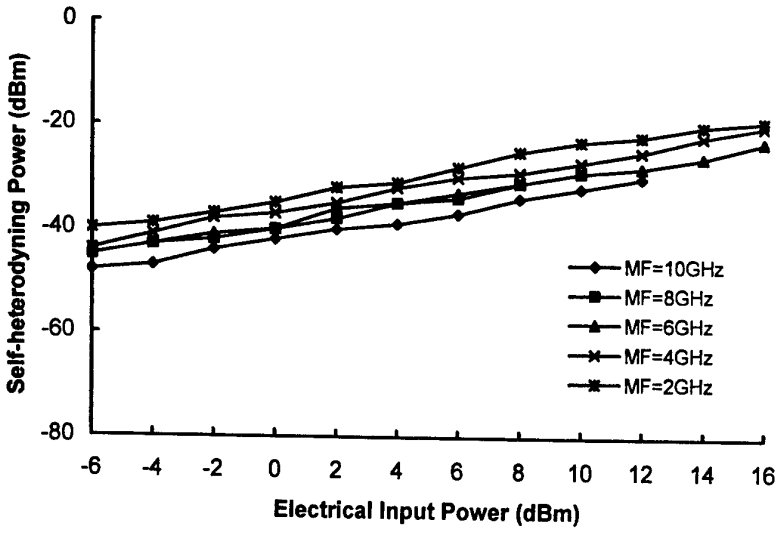

Figure 16: First-order harmonic modulation responses of PM150.

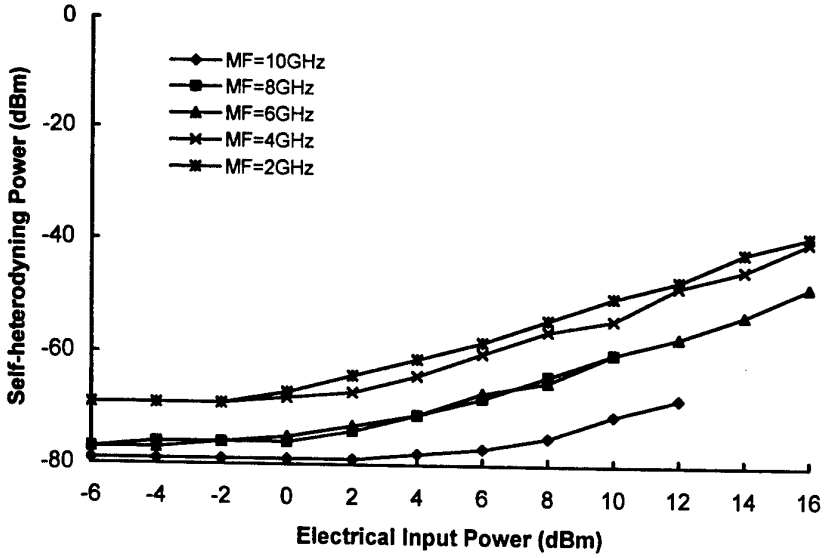

Figure 17: Second-order harmonic modulation responses of PM150.

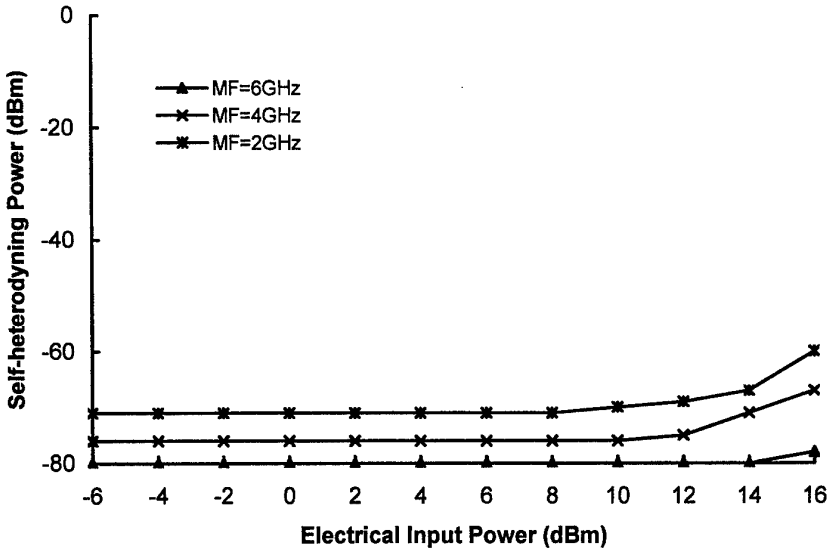

Figure 18: Third-order harmonic modulation responses of PM150.

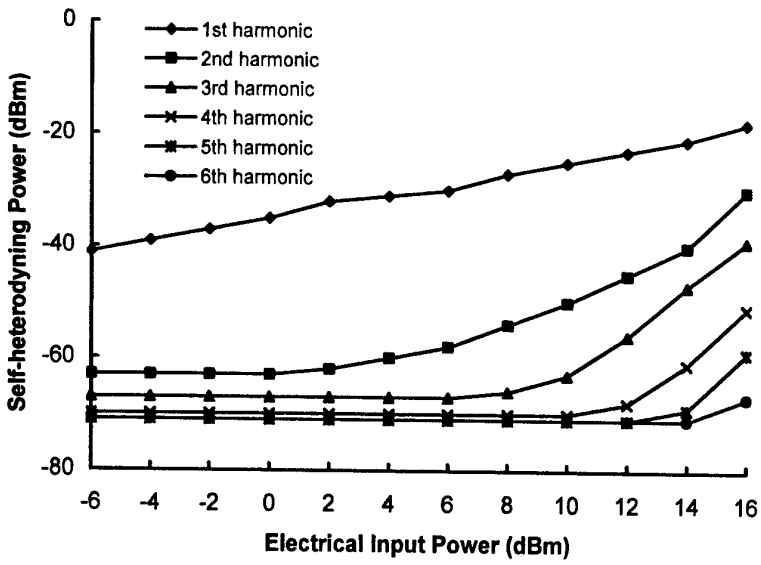

(a) 1 GHz

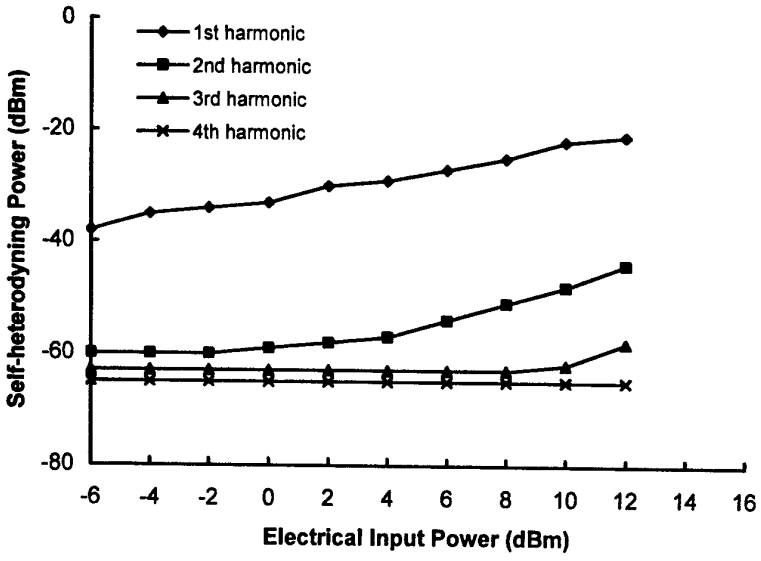

(b) 500 MHz

Figure 19: Low-frequency modulation responses of PM150.

The self-heterodyning method cannot be used to characterise phase modulators near DC, because of the laser self-heterodyning noise and DC-blocking characteristics of the electrical amplifier used. These near-DC characteristics of the phase modulators include both the zero-order and low-frequency modulation responses. To overcome this near-DC limit, these low-frequency modulation responses can be obtained using Figure 20.

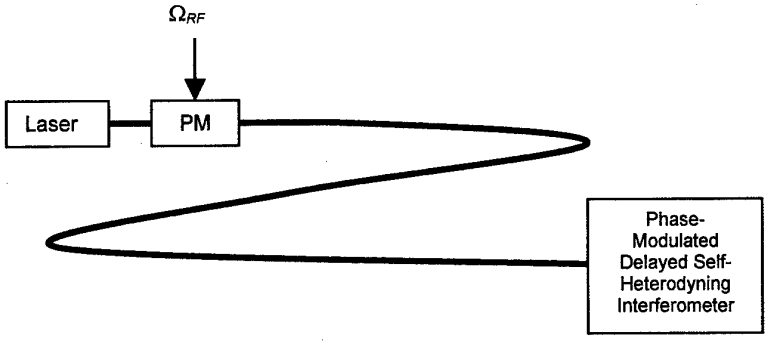

Figure 20: Technique to characterise zero-order and low-frequency responses of phase modulators based on the phase-modulated delayed self-heterodyning interferometer.

The technique shown in Figure 20 would allow the linewidth distribution of the phase-modulated optical carrier to be observed by the interferometer only if the linewidth distribution is replicated to a frequency higher than the modulation frequency under investigation. The experimental arrangement in Figure 20 would also manifest linewidth-broadening properties to be discussed next.

4.3 Linewidth Broadening by External Phase Modulation

By examining Equation 30 for an optical carrier having a general linewidth, $\Delta\upsilon$, the following observations can be made:

1. If $\Omega_{RF} >> \Delta\upsilon/2$, the phase-modulated output would be similar to a frequency-division multiplexed signal. Each of the harmonics resulting from the phase modulation process would have the original linewidth. This is illustrated in Figure 21(a). This is how the arrangement in Figure 20 would allow both the zero-order and low-frequency modulation responses of a phase modulator to be characterised.
2. If $\Omega_{RF} \leq \Delta\upsilon/2$, the overlapping of each harmonic effectively broadens the linewidth of the optical carrier. This is illustrated in Figure 21(a). The extent of the linewidth broadening would depend on the harmonic excitation of a particular phase modulator for a given electrical input condition.

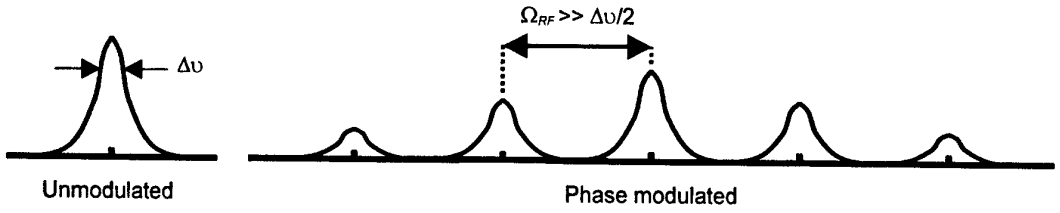

(a) Modulation frequency is large compared to laser linewidth

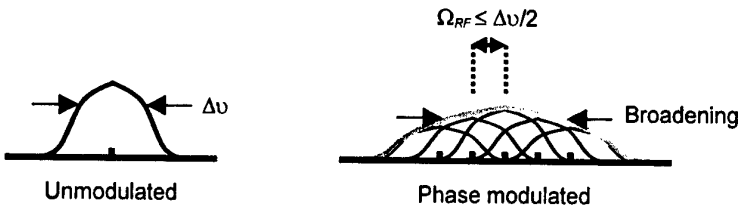

(b) Modulation frequency is small compared to laser linewidth

Figure 21: Conceptual linewidth distribution of a phase-modulated optical carrier.

It is difficult to excite a large number of harmonics in phase modulators for a given electrical input, because the Bessel functions oscillate out of phase with each other. Weak harmonic excitation, i.e. less than a few harmonics, will limit the level of linewidth broadening that can be achieved with the phase modulation technique illustrated in Figure 21(b).

Figure 22 shows a series of self-heterodyning spectra of a DFB laser (Alcatel A 1905 LMI biased at 30 mA) being externally phase modulated (PM150) with electrical input power of 20 dBm. These spectra were obtained using the experimental arrangement shown in Figure 20. The phase modulator in the self-heterodyning interferometer was a Micro Photonix International Corporation 10 GHz device. These spectra demonstrate the behaviour illustrated in Figure 21(a). They exhibit the zero-order components clearly together with other harmonics.

It is worth noting from Figure 21 that the zero-order component of the phase-modulated output is strong at low modulation frequencies (less than 30 MHz), while the first-order harmonics are higher than the zero-order component for modulation frequencies around 50 MHz. This implies that the linewidth broadening by external phase modulation, as shown in Figure 21(b), would be more effective using a modulation frequency near 50 MHz.

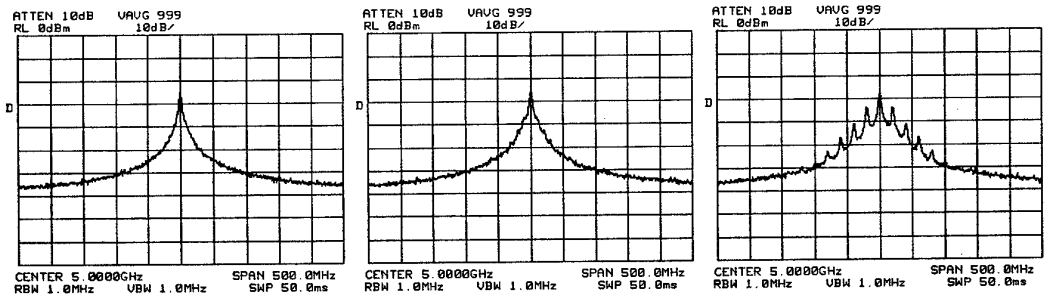

(a) No modulation (b) 10 MHz (c) 20 MHz

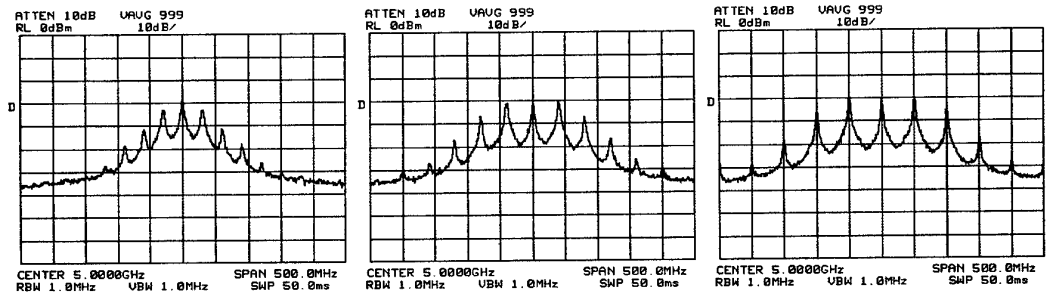

(d) 30 MHz (e) 40 MHz (f) 50 MHz

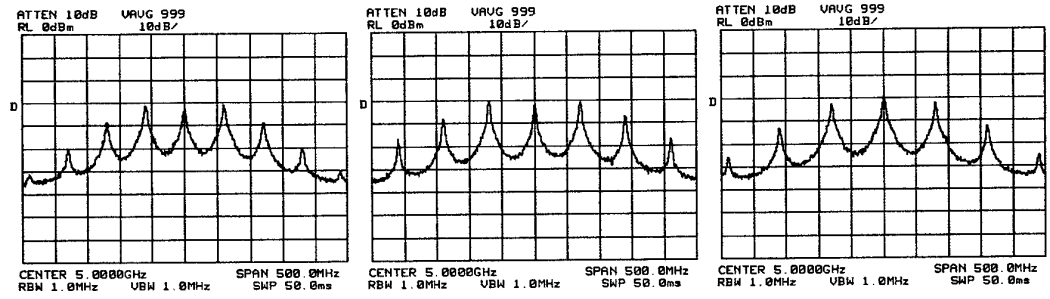

(g) 60 MHz (h) 70 MHz (i) 80 MHz

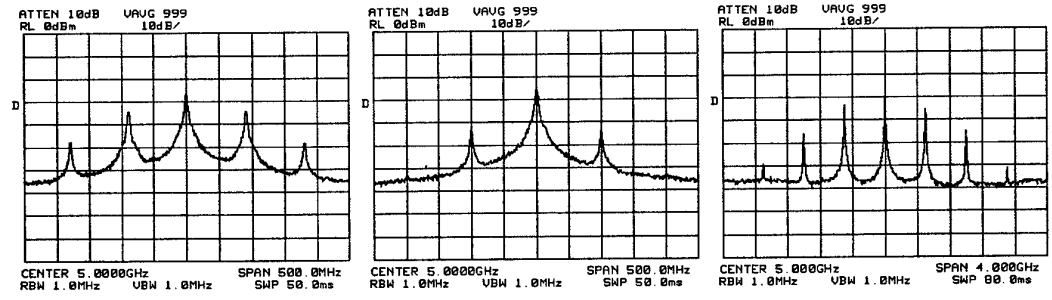

(j) 90 MHz (k) 100 MHz (l) 500 MHz

Figure 22: Self-heterodyning spectra of A 1905 LMI being externally phase modulated at various modulation frequencies.

The tunable laser source (TLS) with coherence control on exhibits a broad linewidth distribution, Figure 11(b), which can be used to confirm the linewidth-broadening technique, as illustrated in Figure 21(b). This was experimentally demonstrated as illustrated in Figure 23. The linewidth distribution was broadened with modulation frequencies in the range of 10-50 MHz. When the modulation frequency of 50 MHz was used, the linewidth distribution was broadened to 200 MHz, i.e. a broadening factor of 2. When the modulation frequency was higher than 50 MHz, which corresponds to half of the full-width of the original linewidth, the linewidth distribution replication no longer overlapped.

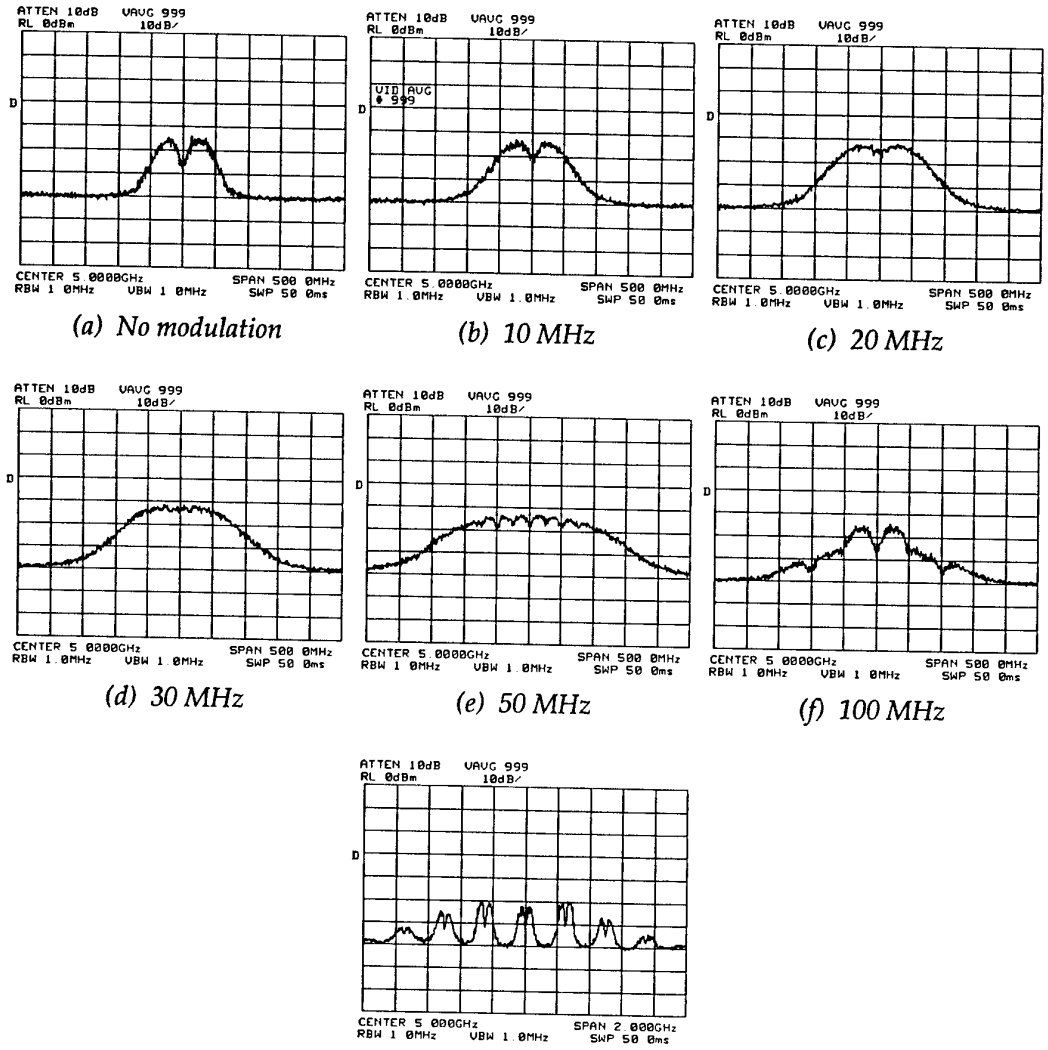

Figure 23: Self-heterodyning spectra of the tunable laser source with coherence control on, being externally phase modulated at various modulation frequencies.

4.4 Summary and Further Discussion

The phase-modulated delayed self-heterodyning interferometer was proposed and successfully used to characterise the responses of an optical phase modulator, i.e. harmonic excitation, as a function of electrical input. While harmonic excitation can be theoretically represented by Bessel functions, actual physical characterisation would provide data on how the harmonics in a particular device are excited for a range of electrical input. Harmonic excitation in a phase modulator would determine how useful it could be utilised to broaden linewidth distribution without affecting the operation of the laser. An experimental demonstration using a COTS phase modulator was successful in broadening a linewidth distribution from 100 MHz to 200 MHz. The broadening factor of this technique strongly depended on the harmonic excitation.

It is interesting to compare the coherence of the unmodulated and phase-modulated outputs of the DFB laser, as shown in Figure 22, in comparison to the linewidth-broadened output from the TLS with coherence control on. A simple differential delay line of 6 metres was constructed with two 50:50 optical couplers. An electrical signal at an arbitrary frequency of 650 MHz was used to amplitude modulate the optical carrier externally. The 650 MHz signal was detected using the spectrum analyser, and the amplitude fluctuation provided a measure of the degree of coherence. 10 dB of fluctuation was observed when no phase modulation was applied, while phase modulation with 50 MHz reduced the fluctuation to around 3 dB. The phase-modulated output from the TLS with coherence control on showed no fluctuation.

It appears that phase modulation does reduce the coherence of an optical carrier. The level of reduction is determined by the linewidth replication due to phase modulation. The phase-modulated output can be considered as an optical carrier with closely spaced wavelengths. Unlike the multi-wavelength optical carrier considered in the Section 3, the overall coherence of the phase-modulated output described above is dependent on the contributions of the narrow linewidth function and the spectral distribution of linewidth replication. This is because closely spaced phase-modulated components are highly correlated as they come from the same laser source.

In order to obtain a smooth broadened linewidth function with external phase modulation, as illustrated in Figure 23(e), the narrow DFB linewidth should be broadened in two stages consisting of injection dithering and then external phase modulation.

A noise source could not be used with the optical phase modulator to perform linewidth broadening. The maximum electrical input power into the optical phase modulator is 27 dBm, which would become very low if it has to be distributed over a wide noise bandwidth. Such low power per Hz would be ineffective, i.e. the harmonic excitation would be low.

5. Linewidth Broadening of DFB Lasers

Using external phase modulation to broaden the linewidth of distributed-feedback (DFB) lasers has its limitations, as outlined in the previous section. It was concluded that in order to obtain a smoothly broadened linewidth function with external phase modulation, the narrow DFB linewidth should be broadened in two stages consisting of injection dithering and then external phase modulation. While this combination seems obvious, the author has not been able to locate any report describing it.

5.1 Wavelength Chirping

The dynamic variation of optical frequency in lasers is referred to as frequency chirping [10]. This term is used interchangeably with wavelength chirping. Ultimately, frequency chirping is a form of internal phase modulation, which can be utilised to broaden laser linewidth. Broadening linewidth by large-signal direct modulation would result in a large-signal modulated optical carrier unsuitable for microwave photonics signal processing. Direct modulation with a noise source would broaden the laser linewidth, but such input noise would consequentially increase the output intensity noise [10]. Therefore, the only alternative for frequency chirping suitable in this work is small-signal direct modulation at low frequencies, which is well known as injection dithering [10]. There are two obvious advantages here:

1. The low-frequency small-signal modulation on the optical carrier would eliminate any problem associated with large-signal modulation. If the small-signal modulation is weak, then the optical carrier can be considered as having constant power in most microwave photonic signal processing applications.
2. The low-frequency modulation could be filtered out in post-detection by electrical amplifiers, which usually have DC-blocking characteristics.

5.2 Injection Dithering

In the investigation of injection dithering, a Fujitsu DFB laser device (FLD5F6CX-H28) was used instead of the Alcatel device (A 1905 LMI), because this device has a suitable dithering capability built-in through its current source. The experimental arrangement is as shown in Figure 24. A voltage function generator provided the injection dithering via Thorlabs LCD-500 current source through the analogue modulation input, which has a conversion coefficient of 50 mA/V. The optical spectrum and linewidth distribution of FLD5F6CX-H28 laser device, biased at 40 mA, are as depicted in Figure 25. It has a measured linewidth of 10 MHz approximately, which compares favourably to the manufacturer's specification of 8-50 MHz. The SRS DS345 function generator provides a lowest output of 0.01 Vpp, i.e. peak-to-peak value. A sinusoidal modulation waveform was used to supply the injection dithering current. Figure 26 depicts a series of self-heterodyning spectra of the Fujitsu laser biased at 40 mA and under various dithering conditions.

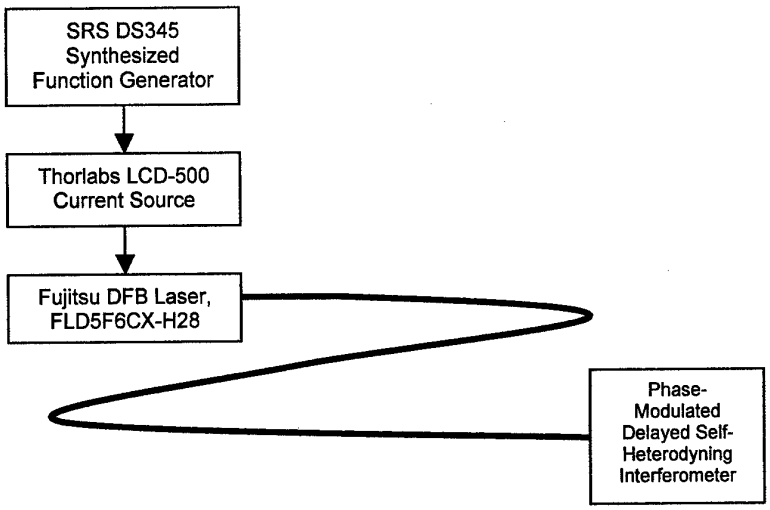

Figure 24: Experimental arrangement for studying injection dithering.

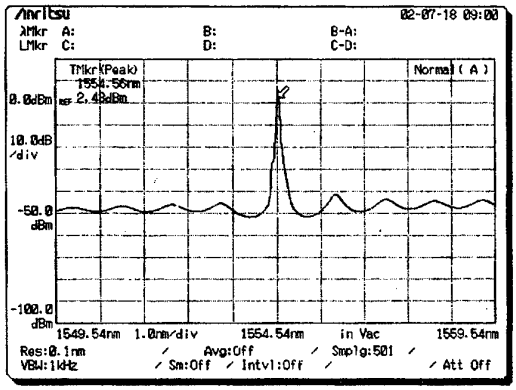

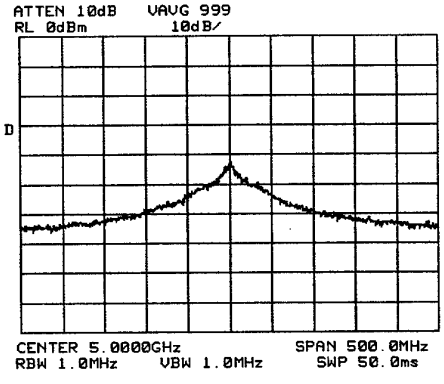

Figure 25: Optical spectrum and linewidth distribution of FLD5F6CX-H28 biased at 40 mA without dithering.

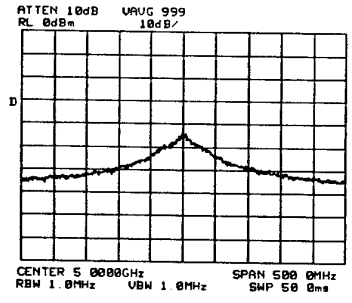

(a) 100 Hz, 0.01 Vpp

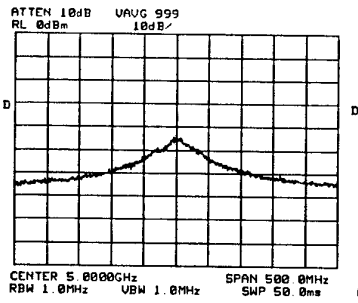

(b) 200 Hz, 0.01 Vpp

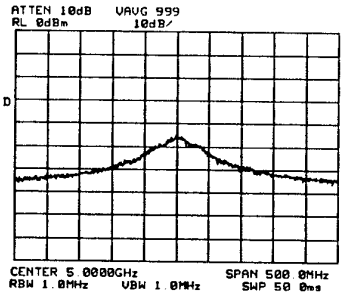

(c) 300 Hz, 0.01 Vpp

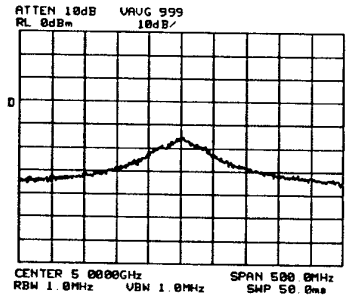

(d) 400 Hz, 0.01 Vpp

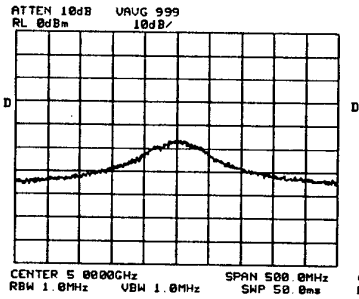

(e) 500 Hz, 0.01 Vpp

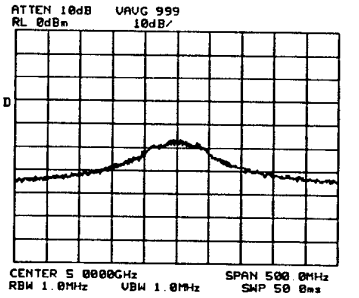

(f) 600 Hz, 0.01 Vpp

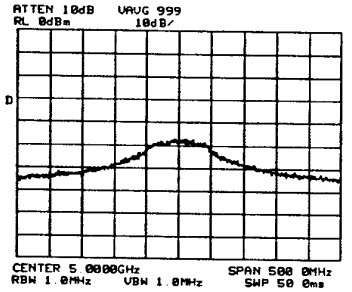

(g) 700 Hz, 0.01 Vpp

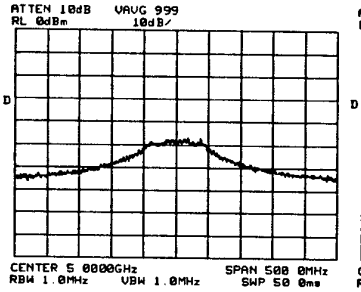

(h) 800 Hz, 0.01 Vpp

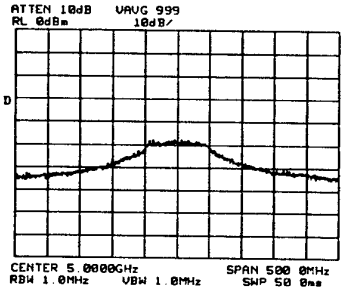

(i) 900 Hz, 0.01 Vpp

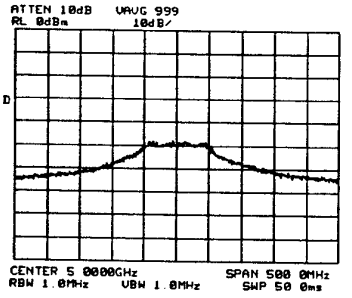

(j) 1000 Hz, 0.01 Vpp

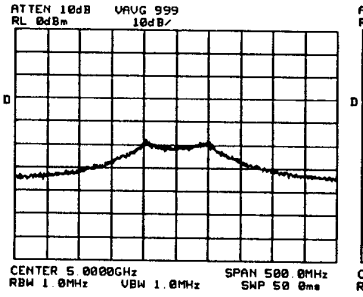

(k) 1500 Hz, 0.01 Vpp

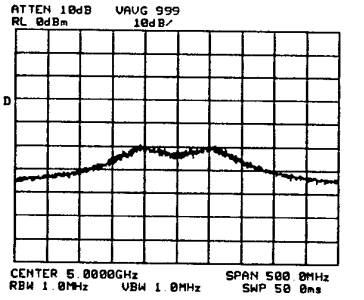

(l) 2000 Hz, 0.01 Vpp

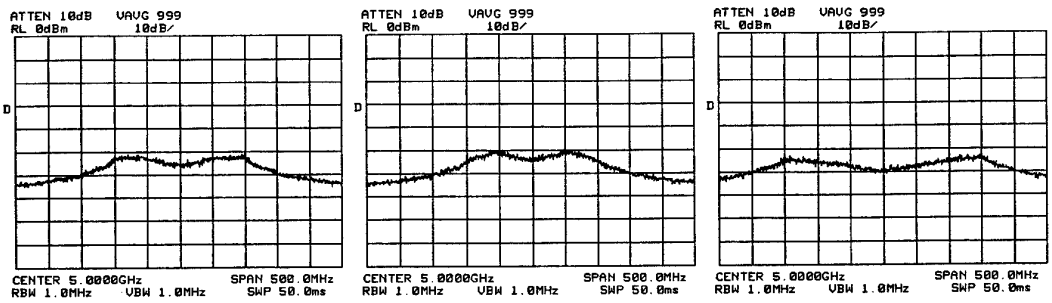

(m) 3000 Hz, 0.01 Vpp *(n) 1000 Hz, 0.02 Vpp* *(o) 1000 Hz, 0.04 Vpp*

Figure 26: Self-heterodyning spectra of FLD5F6CX-H28 biased at 40 mA and being dithered at various sinusoidal conditions.

It can be seen from Figure 26 that if the injection dithering is too weak, in terms of both amplitude and frequency, then the linewidth broadening is minimal, e.g. Figure 26(a) to (c). However, when the injection dithering was strong, the broadening can split the linewidth distribution into two peaks, e.g. Figure 26(k) to (o). Interestingly, the mapping of the broadened linewidth distribution due to injection dithering can be explained and illustrated in the same way as the mapping of a chirped optical spectrum due to large-signal modulation [24].

In this report, the integrity of the broadened linewidth is defined to be the smoothness of its distribution. It is believed that the integrity of the linewidth is best preserved if the injection dithering broadens the distribution, but maintains it as a single-peak distribution, e.g. Figure 26(h) to (j). Equation 17 in Section 2 can be used to define coherence corresponding to a single-peak Lorentzian distribution. When the linewidth distribution becomes multi-peak, as illustrated in Figure 26(k) to (o), then coherence becomes ambiguous. In a two-peak linewidth distribution, it is common to define the linewidth as the frequency separation of the two peaks. Figure 26(j) shows a broadened linewidth of 120 MHz due to injection dithering with 0.01 Vpp at 1000 Hz, as compared to the original linewidth of 10 MHz.

The temporal and spectral (inset) outputs under injection dithering with 0.01 Vpp at 1000 Hz are shown in Figure 27. The optical output was detected with a low-speed photodetector having 1 kΩ transimpedance. The temporal output was recorded with a Tektronix TDS 3045 digital oscilloscope, while the spectral output was taken with a Hewlett-Packard HP9441A vector signal analyser. The 1000 Hz dithering component is clearly modulated on the optical output. However, the peak-to-peak variation of the small-signal modulation is still small compared to the average value. Therefore, such an optical carrier would still be suitable for microwave photonic signal processing when the signals of interest are at MHz and above. Wideband electrical amplifiers in post-detection would filter out the 1000 Hz dithering modulation. However, linewidth broadening means enhancing optical phase noise, which transforms into intensity noise upon detection [10]. Therefore, intensity noise must be analysed systematically.

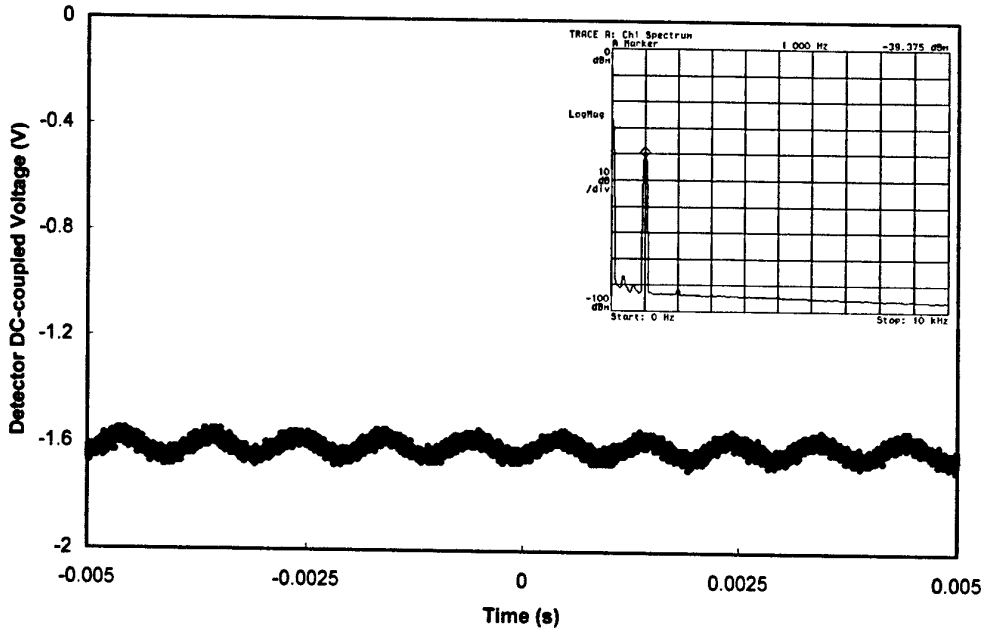

Figure 27: Temporal and spectral (inset) outputs of FLD5F6CX-H28 biased at 40 mA and injection dithered with 0.01 Vpp at 1000 Hz.

5.3 Injection Dithering and External Phase Modulation

Injection dithering successfully broadened the linewidth of a DFB laser from 10 MHz to 120 MHz. This linewidth could be further broadened by utilising external phase modulation.

Figure 28 shows a series of self-heterodyning spectra of FLD5F6CX-H28, biased at 40 mA without dithering, being externally phase modulated at various frequencies. A JDS Uniphase PM150-000738 phase modulator was used. External phase modulation was able to broaden the linewidth distribution at low modulation frequencies as shown in Figure 28(a) to (c). This is due to a significant original linewidth of 10 MHz, as compared to 2 MHz from A 1905 LMI laser device. However, the broadening caused by external phase modulation becomes ineffective at higher modulation frequencies, as depicted by multiple peaks in Figure 28(d) to (f). In fact, the linewidth distribution returned to its original shape when the phase modulation frequency was tuned to around 100 MHz and above. This is due to the strong zero-order component and weak harmonics of the phase modulator.

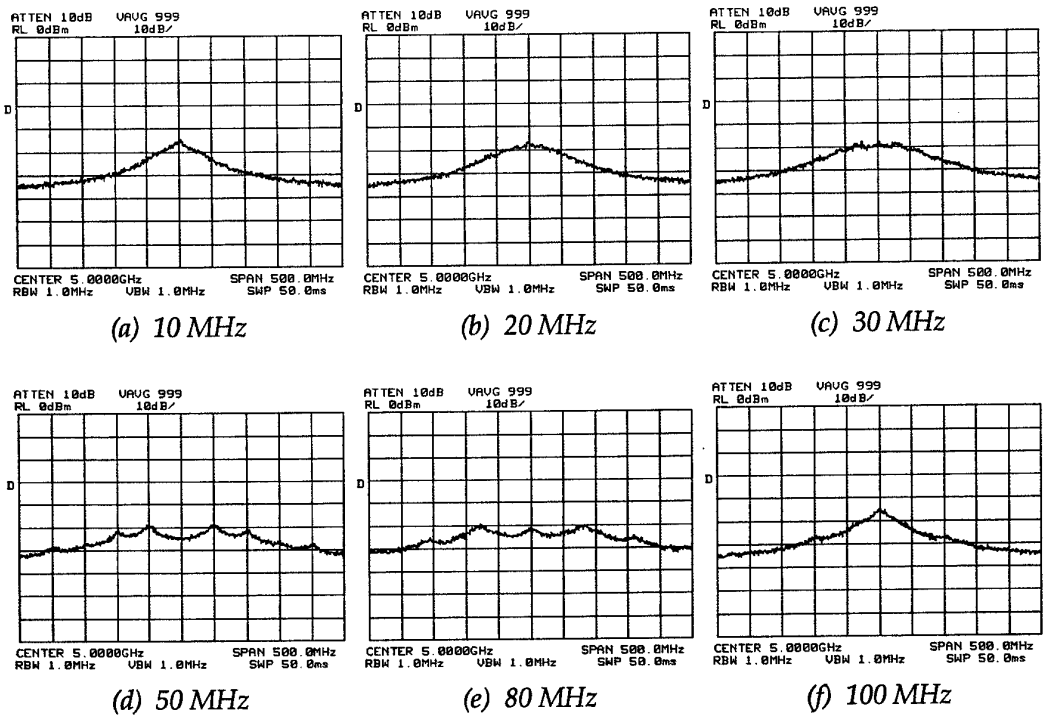

(a) 10 MHz *(b) 20 MHz* *(c) 30 MHz*

(d) 50 MHz *(e) 80 MHz* *(f) 100 MHz*

Figure 28: Self-heterodyning spectra of FLD5F6CX-H28 biased at 40 mA without dithering, being externally phase modulated at various modulation frequencies.

The linewidth of FLD5F6CX-H28 laser device could not be broadened beyond 120 MHz without losing some of the integrity in the linewidth distribution by either injection dithering or external phase modulation. In case of strong injection dithering, it can cause the splitting of the linewidth distribution into two distinct peaks, as shown earlier in Figure 26(k) to (o). For external phase modulation, the integrity of the broadened linewidth distribution is lost at high electrical modulation frequencies, as depicted in Figure 28(d) to (f).

In order to broaden the linewidth beyond 120 MHz, a combination of injection dithering and external phase modulation was proposed and demonstrated. The results are shown in Figure 29. These are the self-heterodyning spectra of the dithered output of FLD5F6CX-H28 with 0.01 Vpp at 1000 Hz, followed by external phase modulation at various frequencies. The combination of injection dithering and external phase modulation was able to broaden an original linewidth of 10 MHz to over 200 MHz, while preserving the integrity of the linewidth distribution, as shown in Figure 29(d). That is an overall broadening factor of over 20, which is double what either injection dithering or external phase modulation alone achieved. Such destruction of coherence corresponds to a reduction in coherence length from 20 m to less than 1 m in optical fibres. However, the effects of intensity noise must be analysed systematically.

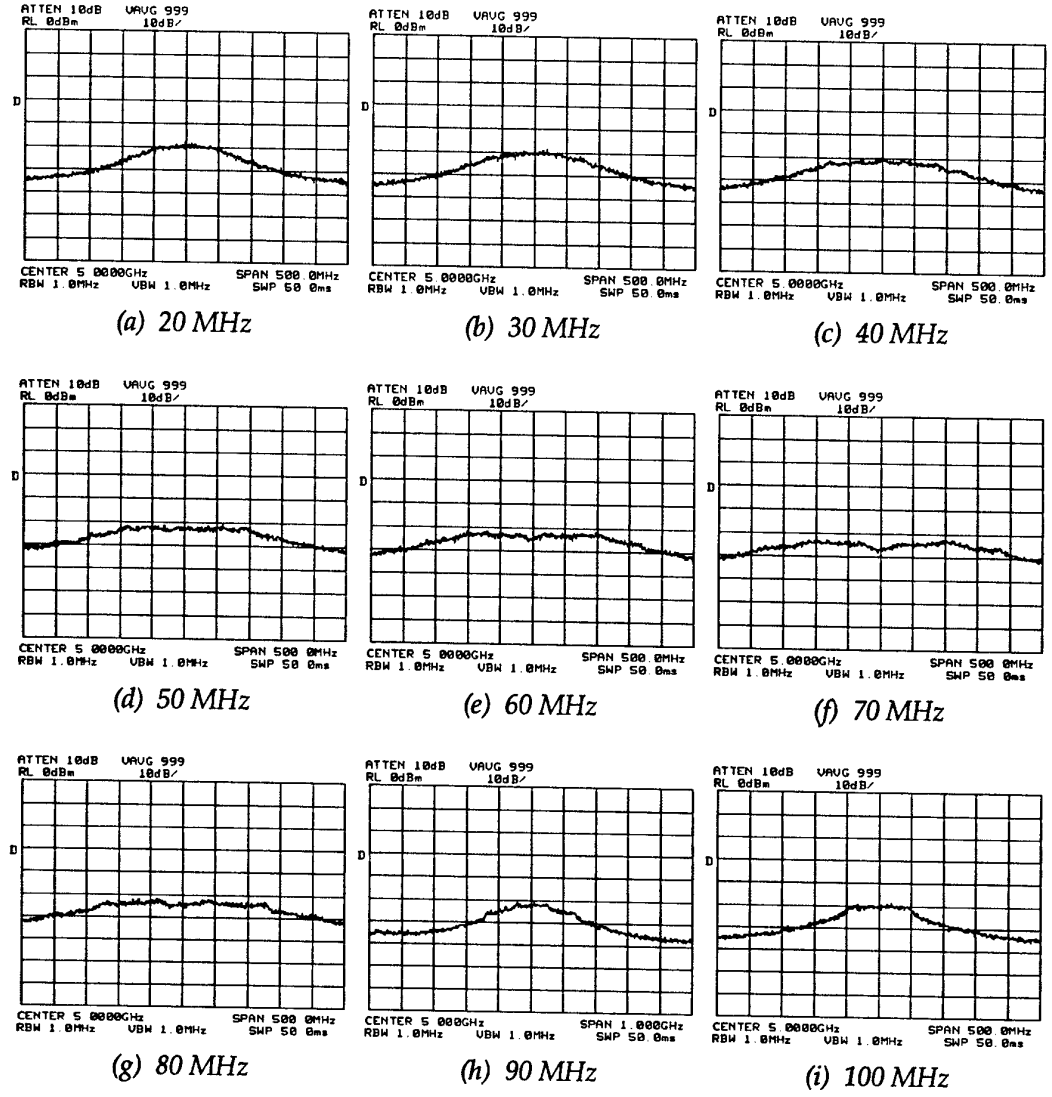

Figure 29: Self-heterodyning spectra of FLD5F6CX-H28 biased at 40 mA and dithered with 0.01 Vpp at 1000 Hz, being externally phase modulated at various modulation frequencies.

5.4 Summary

It has been shown in this section that it is possible to broaden the linewidth of a DFB laser from 10 MHz to over 200 MHz by a combination of injection dithering and external phase modulation. This was double what either injection dithering or external phase modulation alone achieved.

The limitation of this DFB linewidth broadening technique would depend on the following:

1. Susceptibility of frequency chirping to injection dithering, which can be used to broaden the original linewidth, while preserving the integrity of the linewidth distribution.

2. Excitation of high-order harmonics of the phase modulator at the operating electrical input. External phase modulation can perform linewidth broadening more efficiently with strong harmonic excitation.

It may be possible to perform DFB linewidth broadening to ~1 GHz if both the laser device and phase modulator have the right operating characteristics. Nevertheless, it has been shown here that DFB linewidth broadening is possible through a simple technique of injection dithering and external phase modulation, turning these laser devices into compatible sources for microwave photonic signal processing, based on differential delays, in Electronic Warfare systems operating at intermediate frequencies in the order of hundreds of MHz. Other photonic techniques can be employed to process signals at higher frequencies.

6. Conclusions

The major results from the work presented in this report are:

1. The linewidth distribution of a wavelength-division multiplexed optical carrier does not depend on the wavelength distribution or spacing. The phase fluctuation of each wavelength contributes linearly to the overall linewidth distribution.

2. The analysis of linewidth distribution of multi-wavelength optical carrier shows that Fabry-Perot (FP) semiconductor lasers can be either coherent or incoherent. The coherence of FP laser devices is dependent on the phase fluctuation of each longitudinal mode, not the spectral width.

3. External phase modulation can be used to broaden the linewidth of an optical carrier. However, linewidth broadening strongly depends on the harmonic excitation harmonics of the phase modulator at the operating electrical input. The broadening factor was found to be 2 for a commercially available phase modulator.

4. The penalty of using injection dithering to broaden linewidth of distributed-feedback (DFB) laser diodes is a low-frequency small-signal amplitude modulation on the optical carrier. Most microwave photonic signal processors should be able to tolerate such low-frequency small-signal amplitude modulation, which would be filtered out by the DC-blocking electrical amplifiers in post-detection.

5. If the low-frequency small-signal amplitude modulation of the optical carrier is tolerable, then a combination of injection dithering and external phase modulation can be utilised to broaden DFB linewidth beyond what either technique alone can achieve without splitting the linewidth distribution into peaks. The outcome presented in this report shows a 10 MHz linewidth distribution was broadened to over 200 MHz. That is a broadening factor of over 20.

Points 1-4 are known within the laser physics community. They were reported to set a platform to present a new finding in point 5, i.e. using a combination of injection dithering and then external phase modulation to perform linewidth broadening of DFB devices to reduce their coherence for microwave photonic signal processing. While this combination seems obvious, the author was unsuccessful in locating any report describing such a solution. It may be possible to perform DFB linewidth broadening to around 1 GHz if both the laser device and phase modulator have the right operating characteristics. Nevertheless, a simple combination injection dithering and external phase modulation can turn these commercial-off-the-shelf (COTS) DFB laser devices into compatible sources for microwave photonic signal processing.

7. Recommendations

It has been shown in this report that DFB linewidth broadening is possible through a simple technique of injection dithering and external phase modulation, turning these laser devices into compatible sources for microwave photonic signal processing. However, all DFB semiconductor lasers commercially available are targeted at the telecommunication applications, and so not all of them would be compatible for microwave photonic signal processing applications.

It is therefore necessary to undertake a characterisation process to determine the suitability of a particular laser selection to the specific microwave photonic signal processing application, including the ability to broaden the linewidth to a magnitude required by the system specifications. An analysis of the enhancement of intensity noise due to the linewidth broadening process would further improve the understanding of its limitations and application in microwave photonic signal processing.

Recommended future research directions to complement the research outcomes presented in this report include investigating erbium-doped fibre ring laser (EDFRL) configuration as an incoherent multi-wavelength source suitable for microwave photonic signal processing. Understanding all types laser technologies suitable for microwave photonic signal processing applications would provide engineers with alternative design solutions in the development of photonic Electronic Warfare systems.

8. References

[1] D.B.Hunter, "Microwave photonic signal processing using fibre Bragg grating structures", *PhD Thesis at the University of Sydney*, 1999

[2] W.D.Stanley, G.R.Dougherty and R.Dougherty, "Digital signal processing", Prentice-Hall Inc., 1984.

[3] G.A.Ball, W.H.Glenn and W.W.Morey, "Programmable fiber optic delay line", *IEEE Photonic Technology Letters*, **6**, pp. 741-743, 1994

[4] J.Capmany, J.Cascon, D.Pastor and B.Ortega, "Reconfigurable fiber-optic delay line filters incorporating electrooptic and electroabsorption modulators", *IEEE Photonic Technology Letters*, **11**, pp. 1174-1176, 1999

[5] F.Coppinger, S.Yegnanarayanan, P.D.Trinh, B.Jalali and I.L.Newberg, "Nonrecursive tunable photonic filter using wavelength-selective true time delay", *IEEE Photonic Technology Letters*, **8**, pp. 1214-1216, 1996

[6] K-L.Deng, K.I.Kang, I.Glesk and P.Prucnal, "A 1024-channel fast tunable delay line for ultrafast all-optical TDM networks", *IEEE Photonic Technology Letters*, **9**, pp. 1496-1498, 1997

[7] D.B.Hunter and R.A.Minasian, "Tunable microwave fiber-optic bandpass filters", *IEEE Photonic Technology Letters*, **11**, pp. 874-876, 1999

[8] S.Gweon, C.E.Lee and H.F.Taylor, "Wide-band fiber optic signal processor", *IEEE Photonic Technology Letters*, **1**, pp. 467-468, 1989

[9] M.Y.Frankel and R.D.Esman, "Fiber-optic tunable microwave transversal filter", *IEEE Photonic Technology Letters*, **7**, pp. 191-193, 1995

[10] G.P.Agrawal and N.K.Dutta, "Long-wavelength semiconductor lasers", Van Nostrand Reinhold

[11] "Lightwave components & modules databook", Fujitsu Compound Semiconductor Inc., 2001

[12] D.Derickson, "Fiber optic test and measurement", Prentice Hall PTR, 1998

[13] G.L.Koay, "Optical feedback-induced noise in semiconductor lasers", *Master Thesis at the University of Melbourne*, 1994

[14] C.H.Henry, "Theory of the linewidth of semiconductor lasers", *IEEE Journal of Quantum Electronics*, **18**, pp. 259-264, 1982

[15] T.Okugawa and K.Hotate, "Synthesis of arbitrary shapes of optical coherence function using phase modulation", *IEEE Photonic Technology Letters*, **8**, pp. 1710-1712, 1996

[16] Z.He and K.Hotate, "Distributed fiber-optic stress-location measurement by arbitrary shaping of optical coherence function", *IEEE Journal of Lightwave Technology*, **20**, pp. 1715-1723, 2002

[17] T.Saida and K.Hotate, "High-spatial resolution reflectometry by synthesis of optical coherence function for measuring reflectivity distribution at a long distance", *IEEE Photonic Technology Letters*, **10**, pp. 573-575, 1998

[18] K.Hotate, X.Song and Z.He, "Stress-location measurement along an optical fiber by synthesis of triangle-shaped optical coherence function", *IEEE Photonic Technology Letters*, **13**, pp. 233-235, 2001

[19] K.Hotate, "Application of synthesized coherence function to distributed optical sensing", *Measurement Science and Technology*, **13**, pp. 1746-1754, 2002

[20] A.Yariv, "Optical electronics", HRW Saunders, 1991

[21] R.W.Boyd, "Nonlinear optics", Academic Press Inc., 1992

[22] Private communications with Dr. Timothy Priest of Electronic Warfare & Radar Division, Defence Science & Technology Organisation

[23] J.Menders, C.Diamond and E.Miles, "Photonic mm-wave generation using a double passband fiber Bragg grating filter", *Proceedings of SPIE*, **4490**, pp. 63-67, 2001

[24] L.V.T.Nguyen, "Modelling wavelength-dependence of optical gain and ultrafast behaviour in semiconductor lasers", *PhD Thesis at the University of Melbourne*, 1997

DISTRIBUTION LIST

Distributed-feedback (DFB) Laser Coherence and Linewidth Broadening

Linh V T Nguyen

DSTO-RR-0263

AUSTRALIA

DEFENCE ORGANISATION	No. of Copies
Task Sponsor, DGSPD	1
S&T Program	
Chief Defence Scientist	shared copy
FAS Science Policy	
AS Science Corporate Management	
Director General Science Policy Development	
Counsellor Defence Science, London	Doc Data Sheet
Counsellor Defence Science, Washington	Doc Data Sheet
Scientific Adviser Joint	1
Navy Scientific Adviser	Doc Data Sheet
Scientific Adviser - Army	Doc Data Sheet
Air Force Scientific Adviser	Doc Data Sheet
Scientific Adviser to the DMO M&A	Doc Data Sheet
Scientific Adviser to the DMO ELL	Doc Data Sheet
Director of Trials	1
JEWOSU, Squadron Leader Mark Ridley	1
Systems Sciences Laboratory	
EWSTIS (soft copy for accession to EWSTIS Web site)	1
Chief, Electronic Warfare and Radar Division	Doc Data Sheet
Research Leader, EO Electronic Warfare	Doc Data Sheet
Head, EO Technologies	Doc Data Sheet
Dr David Hunter, EWRD,	Doc Data Sheet
Dr Tim Priest, EWRD,	Doc Data Sheet
Dr Kamal Gupta, EWRD,	Doc Data Sheet
Linh V. T. Nguyen, EWRD,	2
DSTO Library and Archives	
Library Edinburgh	1 & Doc Data Sheet
Australian Archives	1
Capability Systems Division	
Director General Maritime Development	Doc Data Sheet
Director General Aerospace Development	Doc Data Sheet
Director General Information Capability Development	Doc Data Sheet
Office of the Chief Information Officer	
Deputy CIO	Doc Data Sheet
Director General Information Policy and Plans	Doc Data Sheet
AS Information Structures and Futures	Doc Data Sheet

AS Information Architecture and Management	Doc Data Sheet
Director General Australian Defence Simulation Office	Doc Data Sheet
Strategy Group	
Director General Military Strategy	Doc Data Sheet
Director General Preparedness	Doc Data Sheet
HQAST	
SO (Science) (ASJIC)	Doc Data Sheet
Navy	
SO (SCIENCE), COMAUSNAVSURFGRP, NSW & Dist List	Doc Data Sheet
Director General Navy Capability, Performance and Plans, Navy Headquarters	Doc Data Sheet
Director General Navy Strategic Policy and Futures, Navy Headquarters	Doc Data Sheet
Army	
ABCA National Standardisation Officer, Land Warfare Development Sector, Puckapunyal	e-mailed Doc Data Sheet
SO (Science), Deployable Joint Force Headquarters (DJFHQ) (L), Enoggera QLD	Doc Data Sheet
SO (Science) - Land Headquarters (LHQ), Victoria Barracks NSW	Doc Data Sheet & Exec Summary
Intelligence Program	
DGSTA Defence Intelligence Organisation	1
Manager, Information Centre, Defence Intelligence Organisation	1
Assistant Secretary Corporate, Defence Imagery and Geospatial Organisation	Doc Data Sheet
Defence Materiel Organisation	
Head Airborne Surveillance and Control	Doc Data Sheet
Head Aerospace Systems Division	Doc Data Sheet
Head Electronic Systems Division	Doc Data Sheet
Head Maritime Systems Division	Doc Data Sheet
Head Land Systems Division	Doc Data Sheet
Head Industry Division	Doc Data Sheet
Chief Joint Logistics Command	Doc Data Sheet
Management Information Systems Division	Doc Data Sheet
Head Materiel Finance	Doc Data Sheet
Defence Libraries	
Library Manager, DLS-Canberra	Doc Data Sheet
Library Manager, DLS - Sydney West	Doc Data Sheet
OTHER ORGANISATIONS	
National Library of Australia	1
NASA (Canberra)	1
UNIVERSITIES AND COLLEGES	
Australian Defence Force Academy Library	1
Head of Aerospace and Mechanical Engineering	1
Serials Section (M list), Deakin University Library, Geelong, VIC	1

Hargrave Library, Monash University		Doc Data Sheet
Librarian, Flinders University		1

OUTSIDE AUSTRALIA

INTERNATIONAL DEFENCE INFORMATION CENTRES

US Defense Technical Information Center		2
UK Defence Research Information Centre		2
Canada Defence Scientific Information Service	(pdf format)	1
NZ Defence Information Centre		1

ABSTRACTING AND INFORMATION ORGANISATIONS

Library, Chemical Abstracts Reference Service	1
Engineering Societies Library, US	1
Materials Information, Cambridge Scientific Abstracts, US	1
Documents Librarian, The Center for Research Libraries, US	1
SPARES	5
Total number of copies:	**32**

DEFENCE SCIENCE AND TECHNOLOGY ORGANISATION
DOCUMENT CONTROL DATA

1. PRIVACY MARKING/CAVEAT (OF DOCUMENT)
UNCLASSIFIED

2. TITLE

Distributed-feedback (DFB) Laser Coherence and Linewidth Broadening

3. SECURITY CLASSIFICATION (FOR UNCLASSIFIED REPORTS THAT ARE LIMITED RELEASE USE (L) NEXT TO DOCUMENT CLASSIFICATION)

Document	(U)
Title	(U)
Abstract	(U)

4. AUTHOR(S)

Linh V T Nguyen

5. CORPORATE AUTHOR

Systems Sciences Laboratory
PO Box 1500
Edinburgh South Australia 5111 Australia

6a. DSTO NUMBER	6b. AR NUMBER	6c. TYPE OF REPORT	7. DOCUMENT DATE
DSTO-RR-0263	AR-012-887	Research Report	September 2003

8. FILE NUMBER	9. TASK NUMBER	10. TASK SPONSOR	11. NO. OF PAGES	12. NO. OF REFERENCES
E 9505-23-159 1	LRR 02/178	DGSPD	44	24

13. URL on the World Wide

http://www.dsto.defence.gov.au/corporate/reports/DSTO-RR-0263.pdf

14. RELEASE AUTHORITY

Chief, Electronic Warfare & Radar Division

15. SECONDARY RELEASE STATEMENT OF THIS DOCUMENT

Approved for Public Release

OVERSEAS ENQUIRIES OUTSIDE STATED LIMITATIONS SHOULD BE REFERRED THROUGH DOCUMENT EXCHANGE, PO BOX 1500, EDINBURGH, SA 5111

16. DELIBERATE ANNOUNCEMENT
No Limitations

17. CITATION IN OTHER DOCUMENTS Yes

18. DEFTEST DESCRIPTORS

Electronic warfare
Semiconductor lasers
Signal processing
Line width

19. ABSTRACT

The primary goal of the research activity presented in this report is to understand the range of applicability for different types of lasers to a variety of Electronic Warfare (EW) applications. This work provides a detailed investigation into laser coherence properties. In particular, the emphasis of this work was on linewidth broadening of commercial-of-the-shelf (COTS) distributed-feedback (DFB) semiconductor lasers, turning them into compatible sources for microwave photonic signal processing. Optical linewidth refers to the optical phase fluctuation of the lasing longitudinal modes. Laser devices having narrow linewidth are said to have a high degree of coherence.

The investigation into laser coherence properties includes linewidth measurements, using a phase-modulated delayed self-heterodyning method, of multi-mode Fabry-Perot (FP) and single-mode DFB semiconductor lasers. Leveraging from these measurements, a combination of injection dithering and external phase modulation is proposed to broaden the linewidth of a COTS DFB laser device. Linewidth broadening from 10 MHz to over 200 MHz is possible without splitting the linewidth distribution, which is often associated with wavelength chirping in semiconductor lasers. The linewidth broadening from 10 MHz to over 200 MHz corresponds to a reduction of laser coherence length from 20 metres to less than 1 metre in optical fibres. The advantages and limitations of the linewidth broadening technique and its applicability to microwave photonic signal processing in EW systems are addressed in this report.